「森林総合研究所研究報告」(Bulletin of FFPRI), Vol.5, No.2 (No.399), 135-174 , June 2006

論　文（Original article）

An experimental study on temporal and spatial variability of flow pathways in a small forested catchment

TSUBOYAMA Yoshio[1)*]

Abstract

This study examined temporal and spatial variability of subsurface flowpaths and sources of streamflow in a small forested catchment. Field investigations were conducted mainly at two different scales: soil to hillslope and hollow to catchment scales. At the soil to hillslope scale, subsurface flow from various portions of a soil profile on a steep, forested hillslope was evaluated by four sets of step-change miscible displacement tests with different application rates and antecedent hydrological conditions. As for hollow to catchment scale, roles of a zero-order basin in catchment hydrology and its internal hydrological processes were investigated by measuring runoff, piezometric heads, and soil temperatures in a zero-order basin (0.25 ha) together with discharges from an adjacent 1st-order basin (0.84 ha) and an entire 1st-order basin (2.48 ha). Results of these investigations indicated that a certain degree of wetness was needed for potential preferential flow paths such as macropores and the axis of a zero-order basin to act as actual flow paths. Once this threshold has been met, each flow path would extend its drainage space by hydrologically linking different locations in space, thus increasing its relative contribution to discharge at a larger scale. This hydrological linkage (and conversely disconnection) which occurs at various scales in the watershed can be seen as a different expression of the variable source area concept. This study associated variations in source areas with potential preferential flow paths which could operate at various scales and revealed processes in which they change their ability as a conduit. Detailed data and analyses presented in this study will enhance our understanding of water transport processes in mountainous catchments and also be useful in watershed management practices through validation and improvement of distributed hydrological models.

Key words : catchment hydrology, zero-order basin, hillslope, soil profile, macropore, groundwater, tracer

Table of contents

原稿受付：平成 17 年 5 月 9 日 Received May. 9, 2005　　原稿受理：平成 18 年 1 月 20 日 Accepted Jan. 20, 2008

* Department of Soil and Water Conservation, Forestry and Forest Products Research Institute (FFPRI), Matunosato 1,Tsukuba, Ibaraki 305-8687, Japan; e-mail: tsubo@ffpri.affrc.go.jp
1) Department of Soil and Water Conservation, Forestry and Forest Products Research Institute (FFPRI)

1 Introduction

1.1 General background

As represented by the word " 山紫水明 ", blue mountains that literally reflect the vast coverage of greenery and clear water that flows through and from those mountains have been invaluable natural resources of Japan. They have benefited us not only by providing materials necessary for our daily life but also by cultivating our spiritual backgrounds. In reality, among a number of languages, Japanese is noted to have many vocabularies which refer to natural things such as seasons, climates, weathers, landforms, and water (Kindaichi, 1988). This suggests that the nature of Japan is so diverse that our ancestors had deep respect to it.

Compared to large river systems in the continents, channels in Japan are generally steep. Many of them have no middle to lower reaches and often pour directly from their headwater areas into the sea. In addition, precipitation in Japan tends to concentrate during particular periods such as Bai-u, typhoon, and snowmelt seasons. As a consequence of these combined natural conditions, flow of rivers varies so widely both seasonally and inter-annually. Coefficients of river regime in Japan often exceed a thousand, which are much larger than those reported for European and North American rivers (Takahashi, 1982).

Because of limited availability of flat lands, Japan has many socioeconomic activities even in headwater areas where slopes are generally steep. Apparently this trend has been accelerated since the age of high-degree economic growth during 1960s. As a result, relatively local events such as landslides, debris flows, and floods of small rivers can result into serious on-site disasters because of their frequency, while floods and sedimentation of large river systems can also be seriously disastrous but less frequent (National Land Agency, 1998). Moreover, it is noted that seasonal and inter-annual variability of precipitation is recently becoming larger, which in turn instabilizes water supply from headwater areas, while water use in a catchment is continuously increasing due to increasing population, diversifying lifestyles, and expansion of industrial activities (NLA, 1998).

As such, headwater areas are sites of much concern from various viewpoints such as mitigation of natural disasters, conservation of natural resources including water as well as ecological aspects, and establishment of nature-rich areas. Thus, it is an important and emerging task to know how water moves within and through these headwater areas. This is not only because of being a subject of the hydrological sciences but also because flow of water is usually the common vector for transport of all other constituents such as sediments, nutrients, and chemicals. Thus, temporal and spatial variations of water affect biotic and abiotic environments of both headwater and downstream areas.

1.2 An overview on studies in catchment hydrology

1.2.1 Runoff generation

Flow and water levels of rivers and canals have been of a particular concern for those associated with river transportation and agriculture. Some of the earliest attempts to predict their seasonal variations and annual maxima can date back to the era of the four major ancient civilizations (Yamamoto, 1972). However, flood forecasting as an engineering tool is noted to have originated since 1930s when Horton presented his infiltration theory (Chorley, 1978). Horton attributed the origin of stormflow to overland flow that generates over a catchment when rainfall intensity exceeds infiltration capacity of the soil surface (i.e., infiltration-excess overland flow). Coupled with the unit-hydrograph method presented by Sherman, the Horton-Sherman model became a common tool for flood forecasting, which was used over several decades thereafter (Chorley, 1978).

The next advance in catchment hydrology appeared during 1960s with the variable source area concepts (Ishihara and Takasao, 1962; Tsukamoto, 1963; Hewlett and Hibbert, 1967). In this dynamic model, near-channel source areas that contribute to streamflow contract and expand in response to rainfall and water tables fluctuating either seasonally or during a storm. Overland flow is supposed to generate only in these near-channel saturated areas (i.e., saturation-excess overland flow), which is contrasting to the concept of Hortonian overland flow (Anderson and Burt, 1990a).

Behind the variable source area concepts existed the fact that hydrologists during that age were not only interested in rainfall-runoff response of a catchment but also started to infer hydrological processes within the catchment (Anderson and Burt, 1990a). Such inferences were first made for vegetated catchments in the humid temperate zones (Chorley, 1978; Anderson and Burt 1990a). As a result, it appeared that infiltration capacities of the surface soils in these catchments were generally much larger than intensity of rainfall at the sites, suggesting that infiltration-excess overland flow would rather be an exceptional case (Chorley, 1978). Since then the variable source area concepts have been a basic framework to understand catchment hydrology (Bonell, 1993).

Detailed field investigations have also proposed specific mechanisms of stormflow generation in catchments. Studies in moderate to gently sloping basins have cited saturation overland flow and return flow within relatively flat riparian areas as the dominant stormflow generation mechanisms (e.g., Betson, 1964; Dunne and Black, 1970; Eshleman et al., 1993; Elsenbeer et al., 1994). Studies in steeper basins have revealed several other dominant stormflow generation mechanisms including interflow (Ishihara and Takasao, 1962), subsurface throughflow (Tsukamoto, 1963; Hewlett and Hibbert, 1967; Ohta, 1988) and pipeflow (Tsukamoto and Ohta, 1988; McDonnell, 1990; Kitahara, 1993). While significance of each mechanism may differ from site to site, importance of subsurface flow is generally acknowledged as a key process in stormflow generation in vegetated catchments covered with permeable soils (Anderson and Burt, 1990b).

1.2.2 Zero-order basins

Topography of mountainous areas is usually characterized by geomorphic hollows located in the middle to upper parts of slopes. These hollows are known to be recurrence sites of landslides (Tsukamoto, 1973; Dietrich and Dunne, 1978; Okunishi and Iida, 1981; Sidle et al., 1985). Tsukamoto (1973) designated such hollows as zero-order basins since they are located in the upstream of 1st order basins. He also addressed that they should be an important topographic unit for geomorphic evolution in headwater areas (Tsukamoto, 1973).

The failure plane is usually delineated by the surface of bedrock, till, or other hydrological impeding layers at the base or within the soil profile. A number of studies have revealed that during rainstorms groundwater accumulates above these restricting layers in the troughs of hollows (Dunne and Black, 1970; Harr, 1977; Pierson, 1980; Tsukamoto et al., 1982; Megahan, 1983). Dunne and Black (1970) depicted a wedge of groundwater accumulating from downslope to upslope during major rainstorms in an agricultural watershed in Vermont, USA. Later studies with more intensive instrumentation have shown more spatial variability in groundwater response (Anderson and Burt, 1977; Tanaka, 1982; Sidle, 1984). These studies suggest that the groundwater peak may occur simultaneously in the upper and lower portions of the slope with contributions of convergent flow, although groundwater peaks may dissipate more quickly in upper slope locations.

Zero-order basins are also recognized as an important topographic unit in runoff generation (Ohta, 1994). Based on detailed hydrological and geomorphological investigations on Pliocene slopes in Japan, Ohta (1988) pointed out strong association of temporal variation of stormflow with a volume of shallow groundwater that expands and shrinks above the trough of the "hydrological base", depths of which could be determined by portable knocking pole penetration tests. Other studies on steep forested slopes underlain by such a hydrological barrier (Luxmoore et al., 1990; Wilson et al., 1991a, b) revealed that this discontinuity can also facilitate lateral subsurface transport of water, which may be important for cycling of nutrients and transport of contaminants such as herbicides, pesticides, and fertilizers to headwater streams.

1.2.3 Subsurface flow

As results of many detailed field investigations, it is now widely recognized that in vegetated catchments covered with permeable soils subsurface flow would play many important roles in runoff generation, chemical transport, and landslide initiation. Thus, a number of studies have been dedicated to elucidate pathways, mechanisms, and origins of subsurface flow (e.g., Tanaka et al., 1988; Pearce, 1990; Wilson et al., 1990; McDonnell et al., 1990).

In order for subsurface flow to contribute to stormflow generation, water has to move fast enough through the subsurface at least at the base of the slope. Several mechanisms have been presented to account for such rapid transport. By far, presented mechanisms can be classified into two groups. The first group focuses displacement mechanisms of water in the subsurface, which includes (1) translatory flow (Hewlett and Hibbert, 1967), (2) capillary fringe effects (Gillham, 1984), (3) effects of entrapped air in the soil (Yasuhara and Marui, 1994), and (4) pressure wave (Torres et al., 1998). Another group emphasizes contribution of preferential flow pathways such as macropores and soil pipes (Beven and German, 1982; Tsukamoto and Ohta, 1988; German, 1990; Kitahara, 1993; Wang et al., 1993; Uchida et al., 1995). Most of these mechanisms have been presented as results from so called pit studies, which measure outflow through the soil pit face that naturally existed or was excavated at the lower or middle parts of hillslopes (Atkinson, 1978).

In addition to these hydrometric techniques, geochemical techniques which utilize stable isotopes (Pearce et al., 1986; Sklash, 1990; Stewart and McDonnell, 1991) and other chemical attributes of water as trace elements (Eshleman et al., 1993; Elsenbeer at al., 1994) have been applied to infer the origin of subsurface flow. Those studies have proved that "old water" is the major component of stormflow in a catchment where subsurface flow contributes to stormflow generation. This suggests that antecedent subsurface water should be effectively displaced by rainwater in the subsurface. Dominance of old water in stormflow has also been recognized in the catchments where soil macropores and pipes are abundant. It is still of much debate whether such a rapid outflow through soil macropores and pipes is bypassing "new water" or displaced "old water" (McDonnell, 1990).

1.2.4 Modeling studies in catchment hydrology

Transport of water in the subsurface has often been treated as laminar flow through a porous medium, mechanisms of which are described by Darcy’s Law and Richards Equation (Richards, 1931). One of the earliest attempt to model water movement in the soil is a theoretical study by Green and Ampt

(1911), followed by analytical studies by Klute (1952) and Philip (1957) on percolation of water in soils.

The appearance of electronic computers in 1950s made then numerical methods such as finite differential methods (FDM) and finite element methods (FEM) feasible ways for solving Darcy's equation. Since these methods can ideally be applied for any shape of regions with various patterns of initial and boundary conditions, these methods soon became common tools for simulating groundwater flow in many fields (Zienkiewicz and Taylor, 1989). At this earlier stage, however, those numerical methods were applied mainly for flows under saturation since they need to utilize sophisticated but somewhat awkward techniques in order to simulate moving water tables. Such techniques include re-allocation of nodal points and/or mesh regeneration (Neuman and Whitherspoon, 1971; Yamagami, 1977). This awkwardness might preclude application of those methods to hillslope hydrology, because distribution of water in hillslopes is generally variable in both time and space. This limitation was relaxed by Neuman and Witherspoon (1971) for FEM and by Freeze (1971) for FDM, through introducing iterative schemes in solving the non-linear Richards' equation. Notably, a series of numerical studies by Freeze (1971, 1972a, and 1972b) were some of the earliest examples of numerical simulation in association with the variable source area concept (Hino et al., 1989, pp.6-13). Following his studies a number of studies have conducted numerical simulation in an attempt to clarify transport mechanisms of water in the soils and/or to develop "physically-based" models in catchment hydrology.

For instance, Tani (1982) numerically solved one-dimensional Richards' equation to analyze response of water table in the soil profile to infiltration. He also used the same method to infer relationship between outflow from a vertical soil column and catchment discharge as well as effects of evaporation onto outflow recession characteristics (Tani, 1985). As to hillslope scales, two dimensional analyses were widely conducted for longitudinal profiles. Numerical analyses of Suzuki (1984a, 1984b) demonstrated effects of evaporation on the properties of a base-flow recession on small mountainous watersheds. Ohta and Kido (1986) incorporated water uptake by tree roots as a sink term and then suggested that transpiration might affect recession characteristics in a different way from evaporation from the soil surface. Other examples of this type of simulation, i.e., 2-D vertical seepage models, include the studies by Sloan and Moore (1984), Hurley and Pantelis (1985), and Tsuboyama and Sammori (1989). One of the most integrated forms of 2-D vertical models was by Bernier (1985), who applied 2-D vertical seepage models to each hillslope segment and simulated spatial and temporal variations in source areas in a whole catchment. On the other hand, Kubota et al. (1987, 1988), through the application of Richards' equation to a two-dimensional horizontal region, developed a model that simulates runoff from a small watershed as well as spatial and temporal distribution of shallow groundwater within it. Smith and Hebbert (1983) as well as Takasao et al. (1986) presented 2-D vertical seepage model coupled with overland flow model based on kinematic wave theory.

As such, numerical simulation based on Richards' equation has provided basis for modeling studies in hillslope to catchment hydrology. However, application of numerical simulations for hydrological behavior at true catchment-scale is relatively limited, while some studies have challenged against this limitation through improving numerical schemes (e.g., Sharma et al., 1987; Troch et al., 1993; Shiraki et al., 1998). This is partly due to the fact that capability of computing environments is still insufficient for simulating full three-dimensional system of catchment hydrology (Hino et al., 1989, pp.1-5). Also there are a number of critiques against simple use of the equation, particularly with concern to effects of preferential pathways (German, 1990; Davidson, 1985; German and Beven, 1985; Oka, 1986; Ogawa et al., 1992).

Besides extensive efforts to develop detailed "physically-based" hydrological models listed above, much work has been dedicated also to hydrological modeling at larger scales, i.e., for a channel network up to a regional river basin. Examples of this kind of models include TOPMODEL (Beven and Wood, 1983), TOPOG (O'Loughlin, 1986), and SHE (Bathurst, 1986). Because such models generally utilize digital elevation data in which surface topography of a catchment is represent by means of either a rectangular grid, an irregular triangular network, or a set of flow tubes (Moore et al., 1991), they are termed as "topography-based" models (Anderson and Burt, 1990b). In these models, each "pixel" over a catchment is topographically "indexed" in advance and it is assumed that hydrological functioning of pixels having a same index should be similar. A consequence of this index approach is being quasi-steady state which means that much less amount of calculation relative to direct solution of Richards' equation is needed to run such a model (Beven, 1993). Their applicability is usually limited to catchments with steep slopes, thin soils, and plenty of precipitation, all of which lead to predominance of gravity (and, hence, surface topography) on water movement. Nevertheless, topography-based models are thought to be very useful not only as a easy-to-run tool for predicting spatial and temporal distribution of hydrological entities over a catchment but also in organizing our knowledge on catchment scale hydrology, for instance, through linking point-scale phenomena and catchment-scale response (e.g., Kubota and Sivapalan, 1995). In many application of such topography-based models, however, spatial resolution of digital elevation data is not always small enough - sometimes as large as several tens of meters. Thus, processes at sub-grid scale are often forced to be lumped or parameterized (Anderson and Burt, 1990b).

Overall, research efforts in modeling catchment hydrology likely have been dedicated to two objectives: 1) to intra-catchment processes where flow pathways and mechanisms are affected mainly by spatial distribution of soil properties and 2) to inter-catchment processes where temporal and spatial distribution of water and flow is affected by surface topography as well.

1.3 Statement of problems

As noted above, detailed hydrometric measurements provides us with visual understanding of flow paths at the pit face usually excavated at the foot of a hillslope. While these techniques are useful to infer flow pathways at a certain cross-section (i.e., an excavated pit face) on the way of subsurface flow, overall transport processes remain unknown because it is rarely possible to see even a foot ahead of the pit face. Studies that incorporate staining techniques and step-wise excavation (e.g., Noguchi at al., 1997) are exceptional although they are laborious as well as destructive (i.e., not repeatable) and tend to be conducted during dry conditions when actual subsurface flow is minimal (i.e., one may not be looking at actual flow processes).

Geochemical techniques based on concentrations of isotopic or certain chemical tracers in water are thought to supplement the limitation of hydrometric approaches by enabling us to infer origins of outflows or residence times of flow components. However, actual mixing processes are still unknown in many geochemical investigations even though they tried to separate storm hydrographs into several components and to associate them with presumed flow pathways (Christophersen et al., 1990; McDonnell et al., 1991). Simply stated, water mixes where water converges. Such places include the base of the slope, places where soils are relatively shallow, and hollows. Nevertheless, few studies to date (e.g., McDonnell et al., 1991; Tsuboyama et al., 1998) have investigated mixing processes at these spatial scales.

Recently, detailed hydrometric and geochemical investigations have been conducted for relatively planar hillslopes (e.g., Brammer and McDonnell, 1996; McDonnell et al., 1998) as well as for geomorphic hollows (e.g., Buttle and Peters, 1997; Anderson et al., 1997). These studies have advanced our conceptual understanding of specific pathways of subsurface flow as well as their relative contributions to runoff from a certain topographic unit (i.e., a hillslope segment or a hollow) during natural and artificial storms, although interactions among flow pathways remain in question. Furthermore, in such detailed investigations relevance of each pathway and/or topographic unit to catchment hydrology is often poorly understood. For instance, the timing, frequency, and magnitudes of hydrological response of such topographic units would be essential information not only for predicting streamflow generation but also for assessing transport of sediment and/or solutes from headwater catchments over long periods.

1.4 Objectives of this study

With these backgrounds, this study aims to obtain better understanding of processes associated with subsurface transport of water within a small forested catchment. Specifically, attempts are made to infer temporal and spatial variability of flow pathways in a small forested watershed through combined applications of hydrometric and tracer techniques to 1) transport processes of water in the subsurface including soil matrices and macropores, 2) internal processes that affect response of a zero-order basin, and 3) contribution of a zero-order basin to catchment hydrology.

2 General site description

This study was conducted in the Hitachi Ohta Experimental Watershed of the Forestry and Forest Products Research Institute. The site is located in the suburb of Hitachi Ohta City, Ibaraki Prefecture, at a longitude of 140° 35´E and a latitude of 36 ° 34´N, and an altitude ranging from 283-341 m (Fig. 2.1). It is near the east coast of the mainland (Honshu) of Japan and experiences a Pacific Coast climate with two major periods of rainfall: the Bai-u season typically from May through June and the typhoon season from August through October (Fig. 2.2). Annual precipitation at the site averaged 1429 mm over the past 18 years (1981-1998). Monthly mean of air temperatur ranges from 2.4°C in January to 23.3°C in August with an annual average of 12.3°C, based on 5 yr records from 1992 through 1997 (Fig. 2.3). Intermittent snow occurs during the winter months; however, the snow is only a minor component of the hydrological budget. Only sporadic winter snowfall occurs and a persistent snowpack does not develop.

Prior to the 20th century, the watershed was covered with a natural broad-leaved forest. In 1914-1915 the forest was clear-cut and replanted with Sugi (*Cryptomeria japonica*) and Hinoki (*Chamaecyparis obtusa*) by 1920. Hardwood and various understory species coexist in gaps within the conifer forest. From 1985 to 1987, the entire basin except Forest Basin B (hereafter, referred to as HB) was clear-cut again and replanted with the same species. Most of field investigations in this study were performed in this unharvested basin (Photo 2.1).

Detailed topographical map was constructed for HB by field survey. Hillslopes in HB are steep (25 to 45 degrees) with deeply incised perennial channels and narrow riparian corridors (2-3 m). Surficial geology is metamorphic, primarily schist

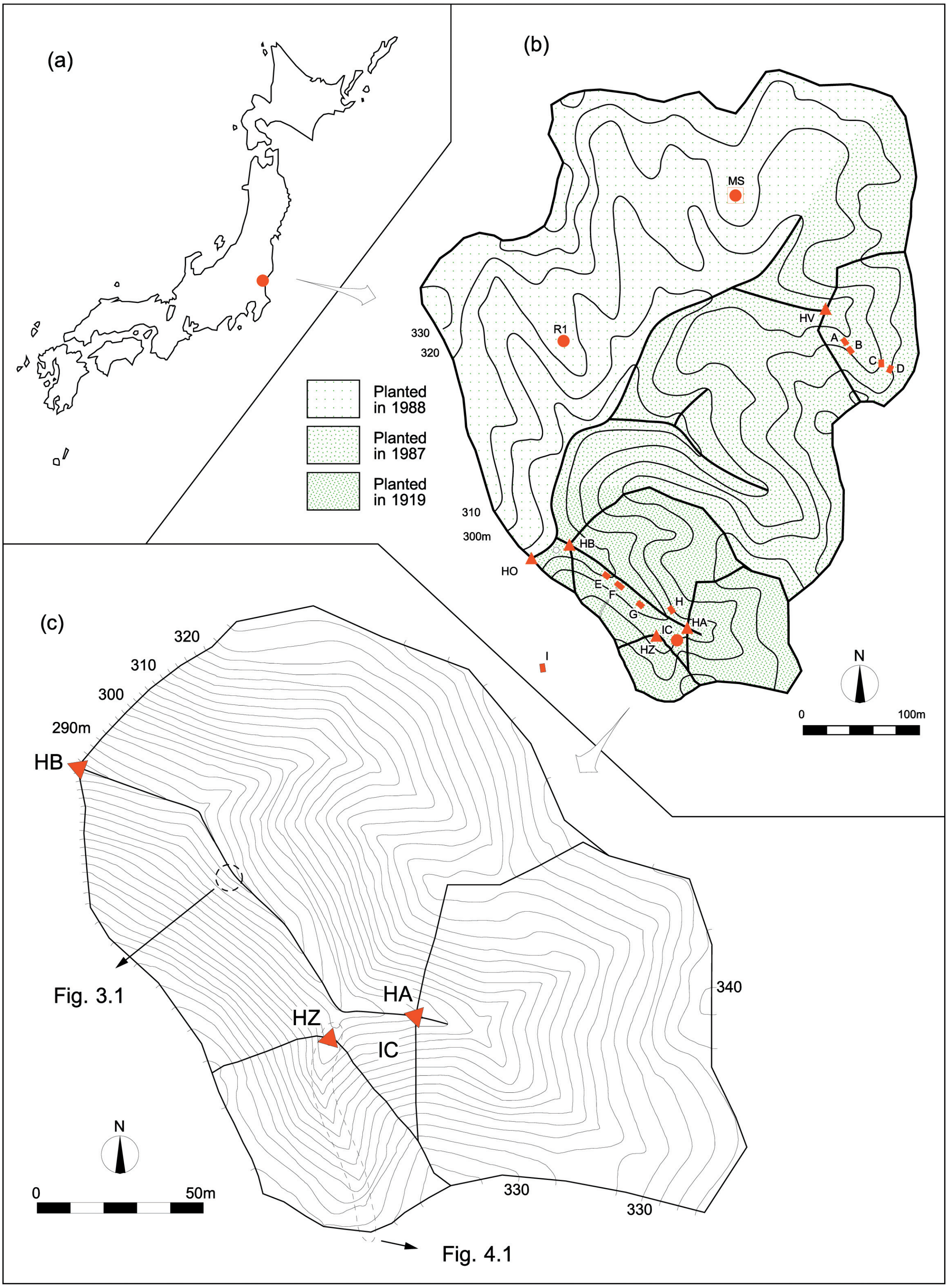

Fig. 2.1 Map of the study site showing (a) its location, (b) topography, vegetation, and instrumentation (HO, HB, HA, HZ, HV: gauging weirs, MS: meteorological station, R1: rain gauges, A-I: soil pit excavated for soil survey), and (c) detailed topography of the three nested drainages investigated in this study.

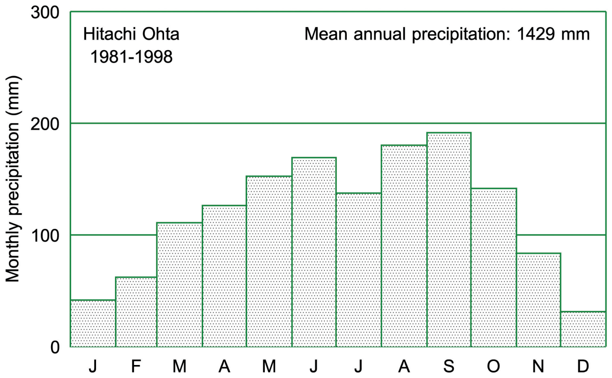

Fig. 2.2 Seasonal variation in monthly precipitation at the site.

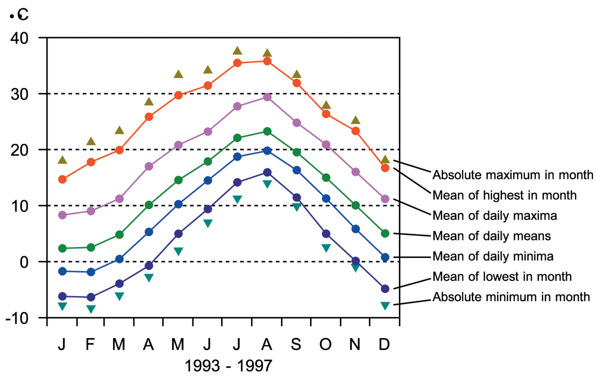

Fig. 2.3 Seasonal variation in air temperature at the site.

Photo. 2.1 An overview of the Forest Basin B (HB)

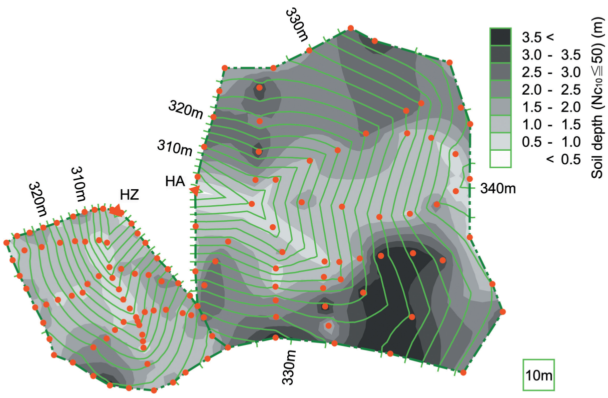

Fig. 2.4 Distribution of soil depths in the subbasins HA and HZ. Solid circles indicate locations where knocking pole penetration tests were conducted.

and amphibolite. Soils are clay loam derived from volcanic ash (Inceptisols) and well aggregated with low bulk densities (0.6 to 1.4 Mg m^{-3}). Saturated volumetric water content and hydraulic conductivities of the soils ranged from 0.52 to 0.86 and from 2.9×10^{-5} to 7.4×10^{-4} m s^{-1}, respectively.

Depth to bedrock or restrictive layer was estimated from knocking pole penetration tests conducted at 180 points mostly in the upstream portion of HB, i.e., in HA an HZ (Fig. 2.4). Sampling points were established according to the surface topography in the field (i.e., not based on an equally spaced rectangular grid). Relationship between depth of soil to bedrock and penetration resistance was preliminarily examined at the soil pits excavated within the watershed. In most cases conversion of results from the penetration tests into soil depth was straightforward. If it was suspected that the restriction might have been a loose rock or a root within the profile, another penetration was made within 1 m of the original point. In this study, depth of soil to bedrock was defined by a criterion Nc=50, where Nc is the number of times of dropping of the weight from the height of 50 cm to drive the cone (diameter = 2.5 cm) 10 cm down into the soil. Depth of the soil in HA and HZ ranged from 0.40 to 4.69 m with an arithmetic mean and standard deviation of 1.61 and 0.90 m, respectively.

3 Soil to hillslope scale variabilities

3.1 Introduction

Subsurface flow in forest soils affects water delivery to streams, water quality, and pore water pressure distribution within hillslope hollows. Recently, the role of subsurface flow in the generation of stream drainage has received much attention (Tanaka et al., 1988; Pearce, 1990; Wilson et al., 1990; McDonnell et al., 1990). Although stable isotope studies have been useful in determining the relative proportions of "old" and "new" water that contribute to streamflow (Sklash et al., 1986; Stewart and McDonnell, 1991), important questions remain as to specific mechanisms and pathways of subsurface flow, particularly in regard to the influence of macropores and the interaction among various hydrological components within the soil. Because of the natural variability in stable isotope concentrations between soil water and groundwater (DeWalle et al., 1988) as well as within and among storm events (McDonnell et al., 1990), other techniques must be utilized to elucidate pathways, travel distances, and quantitative partitioning of subsurface flow within hillslope soils.

Vertical movement of chemicals has been extensively studied in agricultural (Misra et al., 1974; Gaudet et al., 1977; Jury and Sposito, 1985) and forest soils (Sidle et al., 1977; Sidle and Kardos, 1979; Jardine et al., 1990). Both the convective-dispersive equation (e.g., Nielsen and Biggar, 1962; Rose and Passioura, 1971; van Genuchten and Wierrenga, 1986) and stochastic-convection models (e.g., Jury, 1982; White et al., 1986; Hornberger et al., 1990) have been used to simulate the movement of solutes in field soils. Soil structure and the presence of macropore networks are known to influence the transport of chemicals to groundwater (Edwards et al., 1988; Brusseau and Rao, 1990). However, on steep forested slopes underlain by a hydrological barrier, these morphologic features can also facilitate lateral subsurface transport (Luxmoore et al., 1990; Wilson et al., 1991a, b). This lateral movement is important for cycling of nutrients and transport of potential contaminants such as herbicides, pesticides, and fertilizers to headwater streams.

The distribution of pore water pressure within soils of steep hillslope drainages is greatly affected by subsurface flow (Tsukamoto et al., 1982; Tanaka et al., 1988; Sidle and Tsuboyama, 1992). Rather extensive systems of soil pipes caused by subsurface erosion and animal burrows have been described in various areas (Jones, 1971; Pond, 1971; Kitahara et al., 1988). Other types of macropores are smaller and less extensive (Bouma, 1981; Edwards et al., 1989; Edwards et al., 1990; Luxmoore et al., 1990; Schoeneberger and Amoozegar, 1990) and their connectivity depends on their arrangement in space. The extent and continuity of macropore systems may partially control the degree of pore water pressure development in soils during large storms and snowmelt events, thus affecting shallow landslide initiation (Tsukamoto et al., 1982; Sidle et al., 1985). Macropores that are connected over moderate slope lengths in headwater hollows and then become discontinuous are thought to induce regions of pore water pressure buildup (Sidle, 1984).

Forest soils are known to have extensive macropore systems consisting of decayed root channels, earthworm passageways, small animal burrows, subsurface erosion channels, inter-aggregate spaces, and freeze-thaw, desiccation, and tension cracks (Aubertin, 1971; Beven and Germann, 1982). Some macropores, resulting from intermittent episodes of subsurface hydraulic pressure, may gradually become invisible after storms, but still may represent significant preferential flow pathways (Tsukamoto and Ohta, 1988). Luxmoore (1981) designated this intermediate pore class as mesopores - pores that are too small to constitute macropores, yet they serve as preferential flow paths (Luxmoore et al., 1990). Efforts to describe macropore systems in forest hillslopes, particularly with regard to subsurface flow have been limited (Luxmoore et al., 1990; Wilson et al., 1991a, b). Tsukamoto and Ohta (1988) observed that 85.5 to 99.5% of all subsurface flow from a soil profile occurred in soil macropores on Pliocene slopes in Japan. Other investigations have also measured significant contributions of pipeflow to overall subsurface flow in upland drainages (Gilman, 1971; Kitahara and Nakai, 1992).

Soil systems can conceptually be described as having different hydrological components such as matrix and macropore flows. Chen and Wagenet (1992) recently described water movement in an interactive system consisting of macropores within a soil matrix where the extent of the effective macropore system was determined by the antecedent soil water content. Field studies by Roth et al. (1991), in which a chloride tracer was applied for the surface of a vegetable field, indicated that such a two-phase movement occurred for chloride during unsaturated conditions; however, the flow associated with preferential pathways made the overall breakthrough of chloride highly variable. Although some field data are available on the relative hydrological contribution of various portions of the soil profile to subsurface flow (Whipkey and Kirkby, 1978; Wilson et al., 1990; Wilson et al., 1991a, b), few of these data can be evaluated in terms of specific pathways, residence times, and spatial continuity. These factors are all important in terms of streamflow generation, contaminant transport, and pore water pressure buildup.

The objectives of this chapter are to evaluate the relative contributions of various portions of a soil profile (including macropores) to subsurface flow during tests with an applied tracer for different antecedent hydrological conditions. Characteristics of tracer breakthrough curves were used to infer response times of different portions of the soil profile as well as drainage efficiency, including upslope interconnectivity of macropore systems.

3.2 Description and instrumentation of soil pit

Nine soil pits (A to I in Fig. 2.1) were excavated to bedrock at various sites in the watershed (Photo 3.1). Soil profiles were described at each site including the diameter, orientation, continuity, and origin of macropores with diameters ≥ 0.2 cm. Continuity of macropores was examined within an axial reach of 10 cm from the pit face by probing with a thin flexible wire. Soil depth to parent material in the nine pits ranged from 31 to 140 cm with an arithmetic mean of 68 cm (Table 3.1). Average density of described macropores in the profiles was 18.2 m^{-2}. Diameter of described macropores ranged from 0.2 to 4.0 cm with arithmetic and geometric means of 1.22 and 0.89 cm, respectively (Table 3.2). Groups of smaller macropores with diameters less than 0.2 cm were also present but were not described. However, as will be discussed later, those small macropores could also be potential pathways of preferential flow.

Pit F (Fig. 2.1) was prepared and instrumented for subsurface flow measurements (Fig. 3.1). This pit was located at the foot of a hillslope, which was 49 m long with an average gradient of 39°. By locating the pit just upslope of the stream bank and thus simulating a stream bank face, the effects of excavation on the subsurface flow hydrograph and contributing drainage area were minimized (Atkinson, 1978). The soil profile consisted of two major layers: mineral soil (B horizon) overlain by organic-rich soil (organic + A horizons). The pit was 120 cm wide and average soil depth to bedrock was 35.3 cm; however, soil depth varied considerably even within the 120 cm pit width (Fig. 3.1). Depth of organic-rich soil ranged from 3.0 to 7.5 cm (weighted mean of 5.3 cm). Depth of mineral soil ranged from 13.8 to 43.0 cm (weighted mean of 30.0 cm).

Photo. 3.1 A soil pit excavated to investigate distribution of soil layers and macropores.

The pit face intersected sixteen macropores (Fig. 3.2) with diameters ranging from 0.3 to 3.0 cm (Table 3.3). Arithmetic and geometric means of diameters were 0.97 and 0.78 cm, respectively. The included angle between macropore axes and downslope direction ranged from 12° to 84°. Variability in orientation of the macropores may be related to their association with decayed or decaying root channels (Table 3.3). Variability in orientations, together with the discontinuous nature of some macropores (Table 3.3), clearly shows that the macropore networks (and flow paths through them) in the soil are complex and not parallel to the slope.

It was not possible to isolate each macropore because of limited availability of flow measurement instruments. Thus, macropores were lumped into four groups (Table 3.3) and the soil pit was partitioned into five portions (one without macropores), hereafter referred to as C1 to C5, respectively (Table 3.4 and Fig. 3.2). Flow through the soil matrix and macropores of the organic-rich soil layer drained into C1. Three small macropores in the upper left portion of the mineral soil layer drained into C2. Four macropores in the upper right portion of the mineral soil layer drained into C5. The two macropores that drained into C4 were located just above the bedrock. The remainder of the profile (C3) received drainage from the mineral soil matrix excluding macropore flow.

Methods for collecting outflow from various parts of the soil profile are shown in Photo 3.2 and illustrated in Fig. 3.1. Outflow from organic-rich soil including macropores (C1) was collected by inserting a flexible metal sheet with a foam rubber lip between the organic-rich surface layer and mineral soil. The

Table 3.1 Distribution of soil depth within nine soil pits excavated in the Hitachi Ohta Experimental Watershed (A to I in Fig. 2.1).

Layer	Min. cm	Max. cm	Ave. cm	Std. dev. cm
A	3.8	15.0	7.6	3.5
B	19.7	71.0	35.1	15.4
C	0.0	90.7	68.0	31.0
Profile	31.3	140.1	68.0	33.7

Table 3.2 Distribution and size of soil macropores observed in the faces of the nine soil pits.

Layer	Total area	Number of macropores	Density	Diameter of macropores			
				Min.	Max.	Ave.	Std. dev.
	m^2		m^{-2}	mm	mm	mm	mm
A	0.84	21	25	4	30	19	9
B	3.82	103	26	2	40	10	9
C	3.00	16	6	5	40	15	10
Profile	7.66	140	18	2	40	12	10

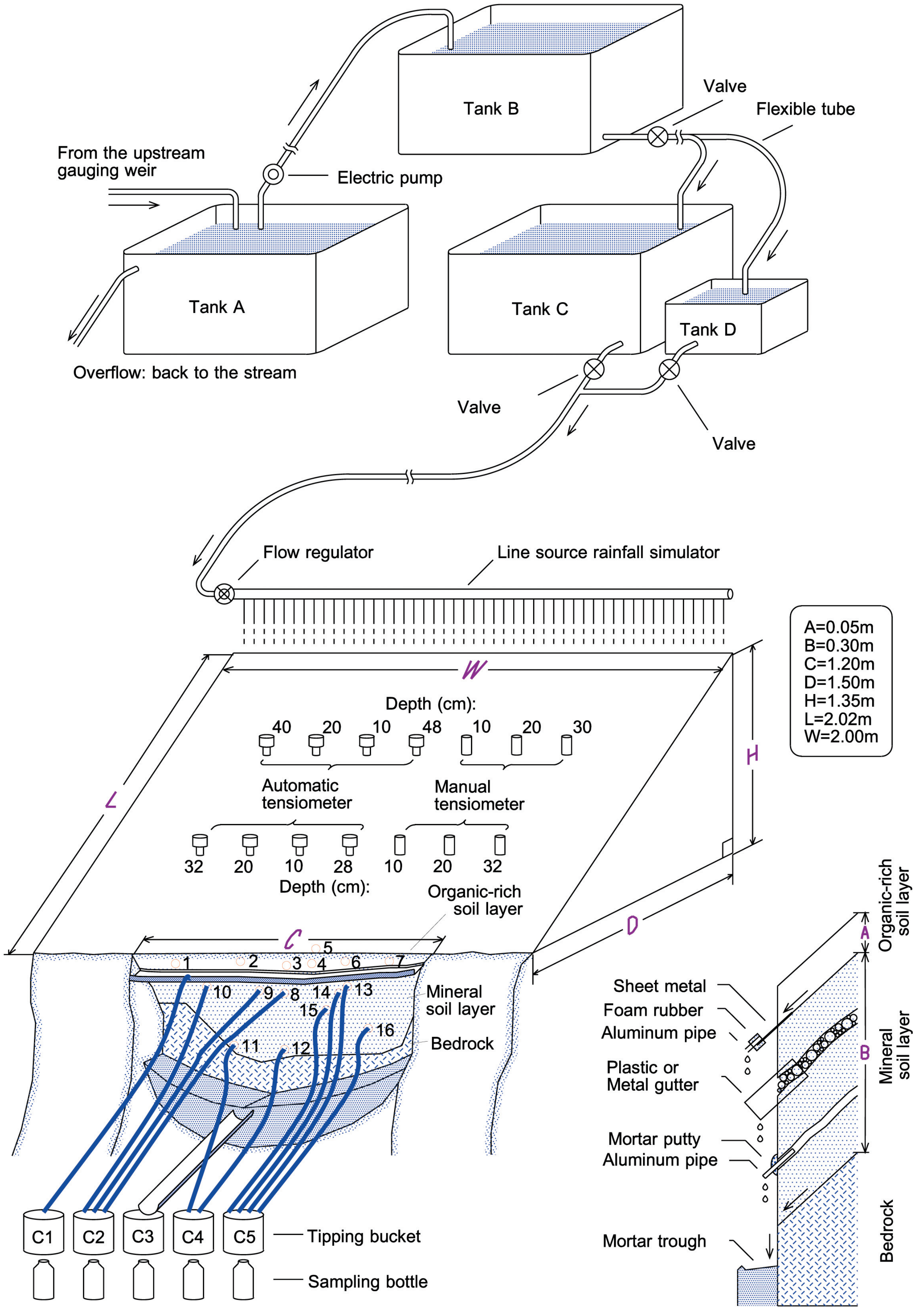

Fig. 3.1 Field diagram for the tracer experiments (Tsuboyama et al., 1994b).

method of collecting water from individual macropores in the mineral soil layer varied. For distinct macropores in non-friable soil (i.e., all four macropores in C5 and one macropore in C4), an aluminum tube with a diameter the same as the macropore was inserted into the macropore and sealed with water-resistant putty (Edwards et al., 1989). For macropores that contained friable soil around their perimeters (i.e., all three macropores in C2 and one macropore in C4), a short piece of plastic gutter was inserted into the soil just below the macropore and water running through the gutter was collected into a funnel. Matrix flow above the macropore was diverted by inserting a small piece of sheet metal. A concrete trough was built into hard bedrock at the base of the pit to collect the remainder of the outflow from the profile (C3). Collectors from the organic-rich soil layer including macropores (C1), the mineral soil matrix (C3), and three groups of macropores (C2, C4, and C5) were connected to five separate tipping buckets and recorders for continuous flow monitoring.

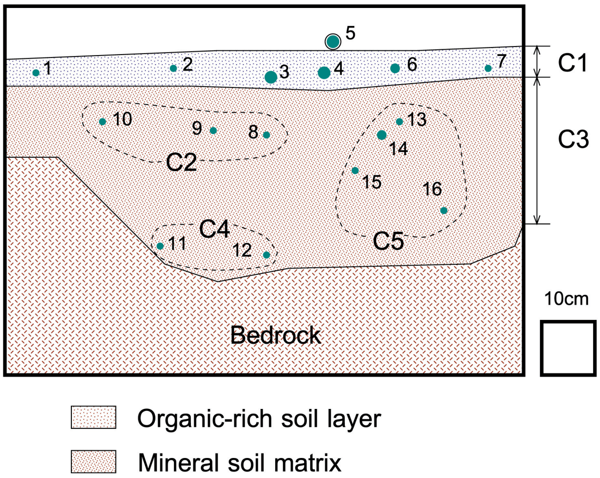

Fig. 3.2 Diagram of soil pit F showing macropore groups and soil horizons.

Automatic recording tensiometers were installed at 0.5 and 1.0 m upslope (lateral distances) from the pit face, at depths of 10, 20, 28, and 32 cm in the lower grid, and 10, 20, 40, and 48 cm in the upper grid, respectively (Fig. 3.1). These eight tensiometers were used to monitor soil water conditions during natural rainstorms and the tracer experiments.

Sixteen soil cores (11.3 cm diameter ×4 cm long) were sampled from the organic-rich and mineral soil layers at pit I, located in a nearby hillslope with similar forest vegetation as HB (Fig. 2.1). A soil water release curve was derived from these soil cores by fitting the theoretical curve (van Genuchten, 1980) to the data obtained from sand column and pressure chamber experiments.

Total volume of pore water within the soil block between the pit face and the irrigation line (Fig. 3.1) was estimated by

Table. 3.4 Partition of the profile in the soil pit F

Portion	Contents	Area in the profile cm2	Percentage %
C1	Organic-rich layer and macropore group 1	636.23	15.02
C2	Macropore group 2	0.71	0.02
C3	Soil matrix	3595.55	84.88
C4	Macropore group 3	1.35	0.03
C5	Macropore group 4	2.13	0.05
Total		4235.97	100.00

Table. 3.3 Description of macropores in the pit F (after Tsuboyama et al., 1994b)

Group number	Macropore number	Diameter cm	Azimuth angle [a] degree	Gradient [b] degree	Included angle [c] degree	Origin
1	1	0.6	64	22	66	(dead end)
	2	0.7	32	-8	36	erosion around root
	3	2.0	60	-38	12	*ditto*
	4	2.0	22	-8	40	*ditto*
	5	3.0	80	36	84	*ditto*
	6	1.0	70	-18	32	*ditto*
	7	0.6	75	-30	27	*ditto*
2	8	0.3	22	-10	38	erosion
	9	0.4	22	-16	33	*ditto*
	10	0.7	83	-1	53	*ditto*
3	11	0.7	0	-37	35	erosion around decaying root
	12	0.8	81	-22	36	decaying root channel(dead end)
4	13	0.9	85	-4	52	erosion
	14	1.0	25	35	79	*ditto*
	15	0.3	40	-15	27	*ditto*
	16	0.5	55	4	47	*ditto*

[a] Defined clockwise starting from the north.
[b] Defined in direction such as gradient of the upslope of the pit would be -42°.
[c] Defined against downslope direction (azimuth=45°, gradient=-42°).

Photo. 3.2 The face of the soil pit F, equipped with devices for outflow measurements.

Photo. 3.3 An overview of the site where tracer experiments were conducted.

multiplying the bulk volume of the soil block by the volumetric water content. The bulk volume of the soil block was assumed to be 635 L, which was the product of the profile area (4236 cm^2 in Table 3.4) and the lateral distance from the profile to the irrigation line (1.5 m in Fig. 3.1). Volumetric water content of the soil block was approximated by averaging water contents at eight points where recording tensiometers were installed. The soil water release curve derived for the soil cores at pit "I" was utilized to calculate water content from the matric potential at each point.

3.3 Experimental procedures

Miscible displacement experiments were conducted at pit F (Photo 3.3). To conduct such an experiment in a field-scale plot, a large amount of water is required. In our study, stream water was diverted by pipeline from the gauging weir of Forest Basin A (HA in Fig. 2.1), about 70 m upstream from the pit. Three large (200 L) plastic tanks and one small (54 L) tank (A, B, C, and D, respectively) were placed upslope of the soil block (Fig. 3.1). During the initial few hours of the experiment, untreated water was applied to the plot. After steady-flow from the pit face was established, a solution of NaCl prepared in tank B with a Cl^- concentration of 1000 mg L^{-1} was applied to the plot until outflow concentrations approached steady-state (i.e., step-change of tracer concentration). Tank C was used to maintain a sufficient pressure head for irrigation. The inclusion of tank D allowed an uninterrupted supply of water to be applied to the plot during the conversion period from untreated to treated water.

The irrigation system consisted of a 2 m line source of intravenous needles (0.7 mm inside diameter) located 1.5 m upslope (lateral distance) from the pit along the contour line (Fig. 3.1). Ninety-six needles were arranged along two closely spaced rows with the needle orifices positioned 2 to 39 cm (weighted mean of 22 cm) above the soil surface (Photo 3.4).

Application rate was checked and maintained by a flow regulator with a flow meter (Photo 3.5). Results of four experiments at application rates of 60 and 90 L h^{-1} (equivalent to 20 and 30 mm h^{-1} of standing water infiltrated over the entire plot area) are reported here and referred to as Runs 1 to 4, respectively (Table 3.5). These application rates are comparable to moderate-intensity storms at the site.

Chloride concentrations in exit water were measured in the field with a Cl^- specific electrode, which was calibrated

Photo. 3.4 An irrigation line source for tracer application.

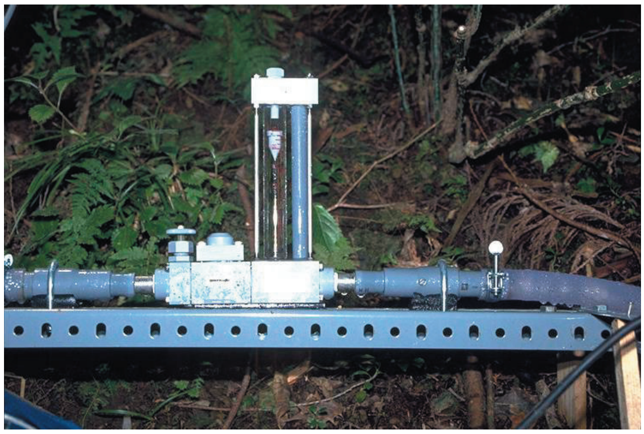

Photo. 3.5 A flow regulator used to maintain steady-state application of water.

about once an hour. Samples of exit water from each portion (C1 to C5) were collected in plastic bottles every 15 minutes during the portion of the tracer test when Cl^- concentration was changing rapidly; thereafter, samples were collected every 30 to 60 minutes. The time interval for each sample collection (0.5 to 5 minutes) depended upon the flow rate with shorter intervals for higher flow rates.

Experimental conditions for Runs 1 to 4 are summarized in Table 3.5. Use of different application rates among these runs reflects mainly attempts to examine its effects on outflow and tracer breakthrough characteristics but also partly resulted from different antecedent conditions which affected water supply.

3.4 Theoretical considerations

The movement of Cl^- in a field soil can be approximated by the one-dimensional convective-dispersive equation for non-interactive solute transport:

$$\frac{\partial C}{\partial t} = D\frac{\partial^2 C}{\partial z^2} - u\frac{\partial C}{\partial z} \tag{1}$$

where C is the Cl^- concentration in solution (mg L^{-1}), D is the longitudinal hydrodynamic (or effective) dispersion coefficient ($cm^2\ s^{-1}$), u is the average pore water velocity (cm s^{-1}), z is the space coordinate in direction of the flow (cm), and t is the time since Cl^- release (s). The initial and boundary conditions corresponding to the step-change miscible displacement in steady-fluid-flow are:

$$\left.\begin{array}{ll} C = C_o; & 0 \le z \le L, t = 0 \\ -D\dfrac{\partial C}{\partial z} + uC = uC_i; & z = 0, t > 0 \\ \dfrac{\partial C}{\partial z} = 0; & z = L, t > 0 \end{array}\right\} \tag{2}$$

where C_o is the background Cl^- concentration (mg L^{-1}), C_i is the input Cl^- concentration (mg L^{-1}), and L is the length of the flow system (cm). Given (2) the approximate solution of (1) would be (Rose and Passioura, 1971):

$$c = \frac{1}{2}\left\{ \mathrm{erfc}\left[\frac{1}{2}\sqrt{\frac{P}{T}}(1-T)\right] + \exp(P)\,\mathrm{erfc}\left[\frac{1}{2}\sqrt{\frac{P}{T}}(1+T)\right]\right\} \tag{3}$$

where c is the relative Cl^- concentration in exit water, T is the number of pore volumes displaced, and P is the Peclet number. These variables (c and T) and parameter (P) are dimensionless and defined as:

$$c=(C_e-C_o)/(C_i-C_o) \tag{4}$$

$$T=ut/L \tag{5}$$

$$P=uL/D \tag{6}$$

where C_e is the Cl^- concentration in exit water (mg L^{-1}).

Theoretical curves based on (3) were fitted to the breakthrough data of individual portions of the soil profile (C1 to C5) as well as to flow-averaged breakthrough data of the entire soil profile. In curve fitting, the number of pore volumes displaced (T) was calculated using the following equation instead of (5):

$$T=Q/V_o \tag{7}$$

where Q is the cumulative outflow since tracer release (L) and V_o is the pore volume (L). Then, average residence time, t_r, was calculated as:

$$t_r=V_o/q_e \tag{8}$$

where q_e is outflow rate averaged over the period of tracer application. Given t_r and P, u and D could easily be calculated from (5) and (6) where T=1 (i.e., t=t_r) and by assuming a certain travel distance (e.g., L=2.02 m). However, u and D are not emphasized in this paper because in this study (1) was mainly used to infer the mixing volume and response time of discrete

Table 3.5 The experimental conditions for Runs 1 to 4.

Experiment		Run 1	Run 2	Run 3	Run 4
Date		Sep 25, 91	Nov 6, 91	Jul 22, 92	Nov 19, 92
Water released		13:00	7:00	7:30	8:30
Tracer released		17:00	9:00	10:00	11:45
Terminated		Sep 26 7:00	17:00	20:00	21:30
Application rate					
	L h^{-1}	60	90	90	60
	mm h^{-1}	20	30	30	20
Antecedent rainfall					
5-days	mm	13.1	0.0	19.0	0.1
10-days	mm	208.1	31.3	43.3	5.9
Soil water content					
1 h before water release		0.487	0.453	0.502	0.476
before tracer release		0.657	0.628	0.630	0.652
after the experiment		0.656	0.651	0.655	0.685
Degree of saturation [a]	%	92	89	90	93
Volume of pore-water [b]	L	417	406	408	425

[a] Average ratio of water content to the saturated water content (0.716) during tracer application
[b] Average value of water content timed the bulk soil volume (635.4 L) during tracer application

portions of the soil profile (i.e., C1 to C5) that were assumed to be represented by V_o and t_r.

As will be shown later, inflow from upslope of the line source appeared to dilute outflow concentrations from individual portions of the profile. For this reason, C_i in (4) was optimized in addition to P and V_o. This was intended to account for the dilution effects by allowing the "input" concentration (C_i) to be lower than the Cl^- concentration in applied water.

Hence, three parameters (V_o, P, and C_i) of the model based on (3) were optimized by minimizing the sum of squares of errors. Parameters were preliminary determined by checking all the possible combinations of parameters within the equally spaced (32×32×32) grid of the range:

$$C_o < C_i \leq C_a$$
$$0 < V_o \leq Q_t \quad (9)$$
$$0 < P \leq 72$$

where C_a is the Cl^- concentration in applied water (mg L^{-1}) and Q_t is the total outflow during tracer application (L). Thereafter, parameters were optimized by the simplex method.

Transport of water and solute in field soils has been thought to be more complex processes than can be represented by the models based on the classic concept of hydrodynamic dispersion (Brusseau and Rao, 1990). For instance, a theoretical study by Matheron and de Marsily (1980) indicates that a convective-dispersive model is inappropriate for stratified media with flow parallel to the bedding. Germann (1991) proposed that the concept of hydrodynamic dispersion only applies if the Peclet number is greater than 32, preferably greater than 72 for a pulse tracer input. Thus, application of (1) is not always justified to simulate solute transport in heterogeneous field soils and consequently the stochastic-convection models have become widely used (e.g., Jury, 1982; White et al., 1986; Beven and Young, 1988; Hornberger et al., 1990).

In our experiment, such parallel flow as Matheron and de Marsily (1980) discussed was not expected to occur because of variability in depths for the surface and subsurface soil layers, random orientation of macropores in the soil, and the line source at the surface of the soil. All of these factors would promote a vertical component in subsurface flow and interchange of flow among various hydrological portions (soil matrix and macropores) within the soil and, hence, longitudinal hydrodynamic dispersion could occur during our tracer experiments. Nevertheless, it has to be emphasized that the application of (1) in this study is basically intended to characterize the transport properties of each portion (C1 to C5) and the entire soil profile, in a framework that has been commonly used.

3.5 Natural hydrological conditions

Based on a 1 yr record through 1992, flow from the soil profile occurred during most natural rainstorms. Outflow characteristics of each portion on an annual basis were summarized in Table 3.6 and outflow response during selected rainstorms is shown in Table 3.7. Flow through the mineral soil matrix (C3) dominates the outflow from the profile in most cases (Table 3.6), since it constitutes 85 % of the pit face area (Table 3.4); however, flows from other portions also contributed to subsurface flow during certain rainstorms (Table 3.7).

Table 3.6 Characteristics of outflow from the profile during rainstorms

Portion	Max. peak flow		Max. outflow[a]		Relative proportion[b]		
					Min.	Max.	Ave.
	$L\ h^{-1}$	$cm\ s^{-1}$	L	$L\ cm^{-2}$	%	%	%
C1	7.23	0.003	283.01	0.44	0.00	23.46	5.25
C2	16.71	6.539	23.82	315.24	0.00	20.35	6.52
C3	98.20	0.008	1749.20	0.49	73.69	100.00	86.52
C4	1.35	0.278	25.01	18.52	0.00	11.87	1.65
C5	0.41	0.053	0.42	0.20	0.00	0.08	0.01

[a] Cumulative discharge during 3 days since a rainstorm or until next rainstorm
[b] Ratio of outflow from each portion to the total outflow from the profile

Table 3.7 Response of discharge from each portion of the profile during two small and a large storms.

Storm date		Aug 1, 92		May 9, 92		Oct 8, 92	
Amount of rainfall (mm)		24.6		23.3		61.4	
10-day antecedent rainfall (mm)		0.3		36.8		57.0	
Duration (h)		13.5		30.5		15.0	
Max. 30 minute intensity ($mm\ h^{-1}$)		15.0		4.4		18.6	
	C1	-	-	0.06	(1.8)	2.83	(0.5)
Peak flow rate ($mm\ h^{-1}$) and	C2	-	-	0.47	(1.8)	15.05	(0.5)
lag time (parenthesized)	C3	7.40	(9.0)	8.80	(1.8)	98.20	(0.5)
from rainfall peak (h)	C4	0.06	(11.5)	0.47	(1.8)	1.23	(2.5)
	C5	-	-	-	-	0.41	(0.5)

Drainage from macropores in upper left portion of the mineral soil layer (C2) was evident during wet hydrological conditions (Table 3.7). Macropores above bedrock (C4) had intermittent flow whereas organic-rich soil layer including macropores (C1) and macropores in upper right portion of the mineral soil layer (C5) had only sporadic outflow. Although C5 consists of macropores in the same soil layer as C2 (Fig. 3.2), drainage from C5 was much less than from C2 (Table 3.6). Additionally, the soil matrix in the upper left portion of the mineral soil profile (near C2) often contributed more free seepage than the remainder of the matrix. These observations imply some interaction between macropores (C2) and the surrounding soil matrix.

While many other investigations have measured significant contributions of pipeflow to overall subsurface flow (e.g., Gilman, 1971; Kitahara and Nakai, 1992), at this site, soil matrix flow was significantly greater than macropore flow (Table 3.6). However, as will be discussed later, evidence of preferential flow pathways was found within the mineral soil matrix (C3) during rainstorms and tracer tests. Different characteristics of outflows among macropore portions (i.e., C2, C4, and C5) indicate that macropores in the soil are not always significant conduits of subsurface flow and degree of their contribution depends on hydrological conditions (Noguchi et al, 2001).

3.6 Experimental results

3.6.1 Outflow characteristics

Hydrographs and tracer breakthrough curves for Runs 1 to 4 are shown in Figs. 3.3 to 3.6, respectively. Characteristics of outflow and tracer breakthrough during four tests are summarized in Table 3.8. Hydrographs and breakthrough curves of C5 are not shown in Figs. 3.3, 3.4, and 3.6 since outflow from C5 was negligible in Runs 1, 2, and 4 (Table 3.8).

Antecedent outflow from the soil profile was highest in Run 1, followed by Runs 3 and 2; no outflow was measured prior to Run 4 (Table 3.8). Just prior to the first three runs, matrix flow accounted for 64.5 to 92.8 % of the total subsurface flow (Table 3.8). The highest discharge (3.51 L h^{-1}) but smallest relative contribution (64.5 % of total outflow) from C3 occurred during Run 1 that had the wettest antecedent conditions (API_{10}=208 mm; Table 3.5). Prior to Run 1, Macropore group C2 comprised

Table 3.8 Characteristics of outflow hydrographs and tracer breakthrough curves during the experiments

Experiment	Portion	Outflow rate				Cl^- concentration	
		Background [a]		Steady state [b]		Background [c]	Final [d]
		L h^{-1}	%	L h^{-1}	%	mg L^{-1}	mg L^{-1}
Run 1	C1	0.000	0.0	7.807	23.6	4	879
Application rate:	C2	1.818	33.4	1.786	5.4	4	349
60 L h^{-1}	C3	3.511	64.5	23.289	70.4	4	764
(20 mm h^{-1})	C4	0.114	2.1	0.213	0.6	4	657
	C5	0.000	0.0	0.002	0.0	-	-
	Profile	5.443	100.0	33.097	100.0	4	765
Run 2	C1	0.000	0.0	1.590	3.4	14	950
Application rate:	C2	0.055	6.6	1.286	2.8	14	907
90 L h^{-1}	C3	0.738	88.3	43.144	93.4	14	892
(30 mm h^{-1})	C4	0.043	5.1	0.204	0.4	14	785
	C5	0.000	0.0	0.000	0.0	-	-
	Profile	0.836	100.0	46.224	100.0	14	894
Run 3	C1	0.000	0.0	3.925	6.1	7	785
Application rate:	C2	0.135	6.4	6.608	10.4	7	731
90 L h^{-1}	C3	1.950	92.8	52.741	82.6	7	773
(30 mm h^{-1})	C4	0.016	0.8	0.079	0.1	7	400
	C5	0.000	0.0	0.485	0.8	7	811
	Profile	2.101	100.0	63.838	100.0	7	769
Run 4	C1	0.000	-	0.818	2.0	9	873
Application rate:	C2	0.000	-	1.144	2.8	10	928
60 L h^{-1}	C3	0.000	-	37.375	92.0	18	902
(20 mm h^{-1})	C4	0.000	-	1.311	3.2	11	906
	C5	0.000	-	0.003	0.0	-	276
	Profile	0.000	-	40.651	100.0	17	902

[a] Values averaged from 6 to 2 h prior to water application
[b] Values averaged over the period of tracer application
[c] Values prior to tracer application
[d] Values at the end of tracer application

33.4 % of the antecedent subsurface discharge although no antecedent drainage occurred in the organic-rich soil (C1). Even during these wettest antecedent conditions, the soil profile was not totally saturated from the bottom as evidenced by tensiometric readings (Table 3.5). Instead, isolated portions of the soil profile (such as around C2) were experiencing saturated flow. During the dry conditions preceding Run 4 (API_{10}=6 mm), no discharge occurred from any portion of the profile (Table 3.8). Antecedent discharge from the soil matrix (C3) appeared to increase proportionally to increasing antecedent rainfall, while outflow through macropore groups exhibited relatively larger variations between wet and dry antecedent conditions.

Volumetric water content was almost constant (0.66) as determined from tensiometers during tracer application in Run 1, while it ranged from 0.63-0.65, 0.63-0.66, and 0.65-0.69 during tracer application in Runs 2 to 4, respectively (Table 3.5). These values are roughly close to 0.72, the saturated volumetric water content. Total volume of pore water within the soil block averaged over the period of tracer application was 417, 406, 408, and 425 L for Runs 1 to 4, respectively. This pore-water volume was calculated by multiplying the bulk volume of the soil block (4236 cm^2 x 2.02 m; see Fig. 3.1 and Table 3.4) by the volumetric water content. Although these values are merely estimates, they indicate that tracer was applied in nearly saturated conditions for all tests. In addition, total volume of pore water was almost identical between the four tests in spite of the different antecedent conditions and application rates. Hornberger et al. (1990) similarly found little variation in pore water volume and nearly saturated conditions during different water application rates on a forested soil block.

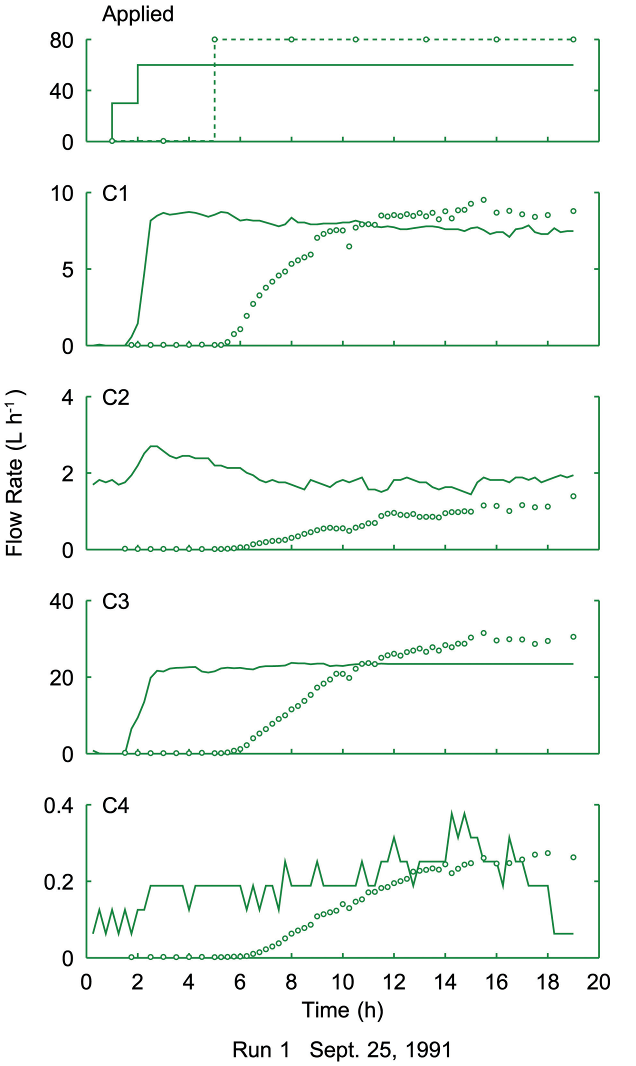

Fig. 3.3 Hydrographs (solid lines) and chloride tracer breakthrough curves (circles) from various portions of the profile during Run 1 (Tsuboyama et al., 1994b).

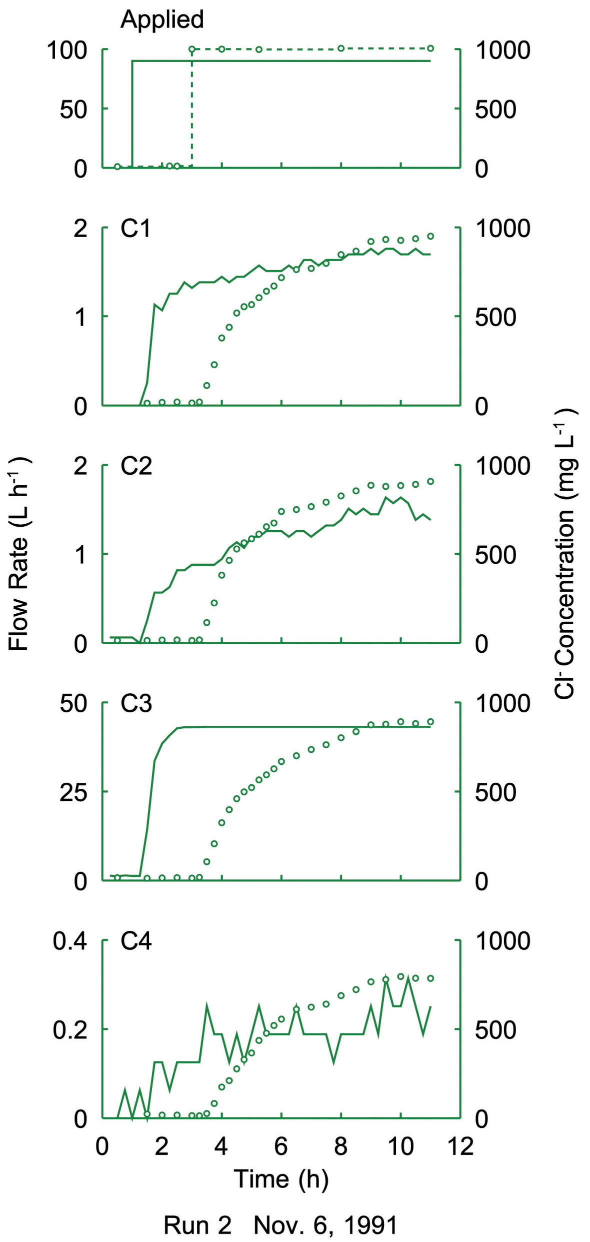

Fig. 3.4 Hydrographs (solid lines) and chloride tracer breakthrough curves (circles) from various portions of the profile during Run 2 (Tsuboyama et al., 1994b).

During tracer application in the first two tests (Runs 1 and 2), the tipping bucket of C3 ceased sending pulse signals to the recorder. This appeared to be caused by shorting of the electrical circuit from sodium chloride in effluent and not due to overflow. In Run 1, insulation of the tipping bucket for C3 shorted 6.5 h after tracer release. Thus, outflow rates from C3 after 6.5 h were extrapolated. In Run 2, breakdown occurred 0.5 h after tracer release. During the remainder of this test, outflow rate was manually monitored by counting number of tips during 30 seconds at least once an hour. The manually monitored outflow rate from C3 was 43.14 L h^{-1} with standard deviation of 1.47 L h^{-1}. This small standard deviation indicates that the outflow rate from C3 was fairly stable.

In all tests, steady-state flow was established before tracer release (Figs. 3.3 to 3.6). Comparing outflow rates before and during water application, total outflow rate from the profile became 6.1 times larger in Run 1, while it became 50 times larger in Run 2 and 30 times larger in Run 3, respectively (Table 3.8). Different response may be attributed to different contribution of inflow from upslope. Ratios of increase in total outflow (above the background level) to application rates were 0.46, 0.50, 0.71, and 0.67 for Runs 1 to 4, respectively (Table 3.8). The ratios are roughly around 0.6, which is the ratio of the pit width (1.2 m) to the length of the irrigation line (2 m). These ratios provide indirect evidence of conservation of applied water. Only -14 to +11 % of the applied water was

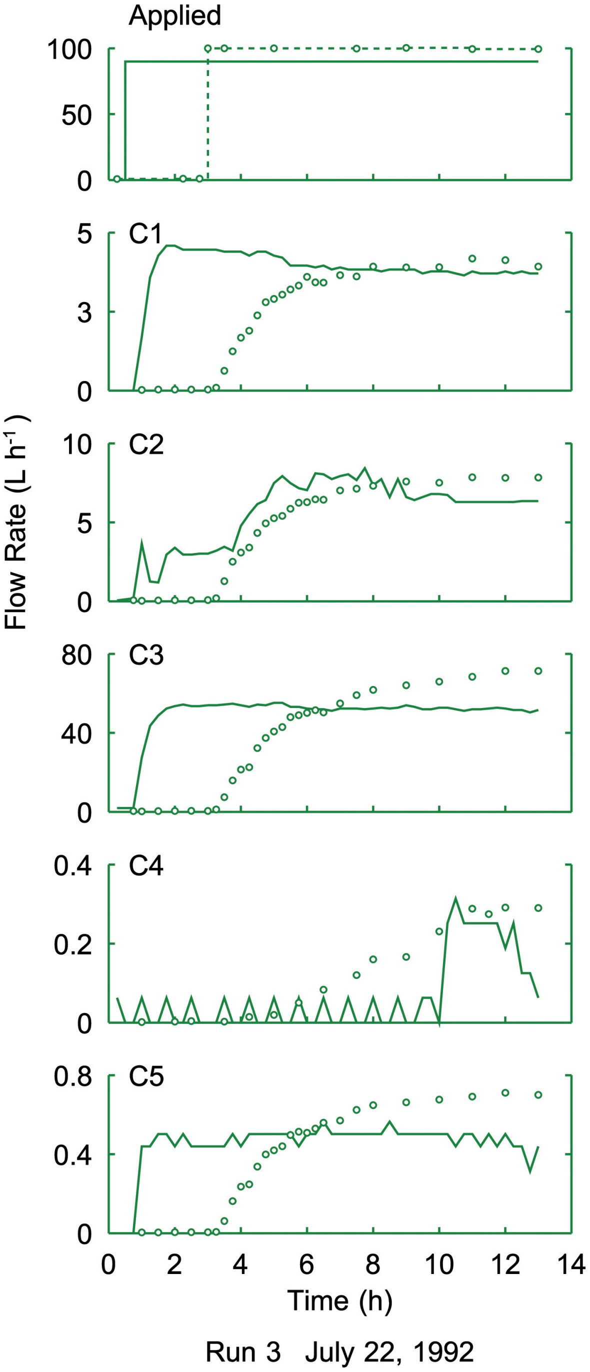

Fig. 3.5 Hydrographs (solid lines) and chloride tracer breakthrough curves (circles) from various portions of the profile during Run 3.

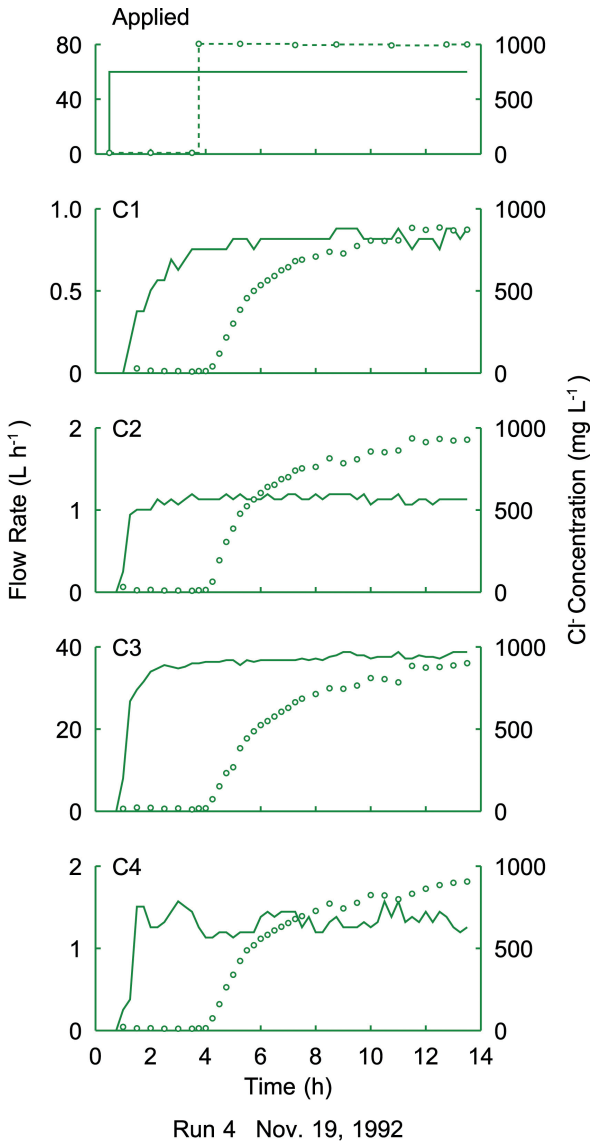

Fig. 3.6 Hydrographs (solid lines) and chloride tracer breakthrough curves (circles) from various portions of the profile during Run 4.

unaccounted for, which is reasonable for field scale conditions.

During tracer application in Runs 1 and 3, flow from the mineral soil matrix (C3) constituted 70 and 83 % of the total outflow from the profile, respectively, while it constituted 93 and 91 % in Runs 2 to 4, respectively (Table 3.8). Relatively higher contribution of C3 seems to reflect wetter antecedent conditions (Table 3.5) rather than difference in application rates (Table 3.8).

While average outflow rate from C3 during application did not vary largely among the four tests, average outflow rate from C1 (the organic-rich soil layer including macropores) during tracer application varied as much as 10 times between the smallest case (Run 4) and the largest case (Run 1). Possibly applied water could more easily bypass the organic-rich layer (C1) and enter the mineral soil (C3) during the driest conditions in Run 4 because of the smaller inflow from upslope into C3 (Table 3.8).

Average outflow rate from C2 (macropores in upper left portion of the mineral soil layer) was much higher in Run 3 than in other runs. During Run 1, outflow rate from C2 decreased slightly after water application, suggesting that applied water changed the relative contribution of individual portions (C1 to C5) of the profile to subsurface flow.

There was little difference in average outflow rate from C4 between the first two tests. A notable increase in outflow occurred in C5 (a group of macropores just above bedrock) and a coincided decrease in C4 (another group of macropores just above bedrock) during Run 3 compared with other runs (Table 3.8). During Runs 1, 2, and 4, there was negligible outflow from C5. The inconsistent nature suggests that these changes cannot be totally associated with different hydraulic loadings. Such changes may reflect new macropore development, macropore clogging and closure, or changes in upslope connectivity.

3.6.2 Tracer breakthrough characteristics

With the exception of C2 in Run 1 and C4 in Run 3, tracer breakthrough curves exhibited a rapid initial increase with extensive tailing (Figs. 3.2 to 3.6). During Run 1, tracer breakthrough was most rapid in organic-rich soil layer including macropores (C1) followed by mineral soil matrix (C3) (Fig. 3.3). Outflows from macropores (C2 and C4) during Run 1 had lower concentrations than outflows from the mineral soil matrix (C3). During Run 2, tracer breakthrough from all portions of the profile approached steady state within 6 h after tracer release (9 h in Fig. 3.4). Also during Runs 3 and 4, tracer breakthrough from most portions approached steady state, likely with slightly longer time for the drier conditions (Run 4). Tracer breakthrough from C4 in Run 3, together with outflow from it, responded erratically.

Outflow from C2 should intuitively have higher tracer concentrations than C4 since macropores of C2 are closer to the soil surface source. However, tracer concentration in outflow from C2 during Run 1 was less than from C4. During Run 1, Cl^- concentrations from C2 did not reach half of the concentration in applied water (Fig. 3.3). This is attributed to the higher flow rates through macropores in C2 from upslope that serve to dilute the outflow concentrations.

3.7 Breakthrough analyses

Experimental and theoretical breakthrough curves are compared in Figs. 3.7 to 3.10 for Runs 1 to 4, respectively. Parameters obtained by curve fitting are shown in Table 3.9. Average residence time for one pore volume calculated for the breakthrough data of C2 in Runs 1 and 3 is large compared to values of other portions (Table 3.9). This difference in t_r may be due to the non-steady characteristics of either the outflow or the Cl^- breakthrough data for C2 (Figs. 3.3 and 3.5) during these wet hydrological conditions (Table 3.5).

Theoretical curves fit experimental data slightly better for Runs 2 and 4 (i.e., drier conditions) than for Runs 1 and 3 (i.e., wetter conditions) although all curves have high correlation coefficients ($r > 0.98$) (Figs. 3.7 to 3.10). The deviation of the theoretical curves from experimental data in Run 1 may be attributed to variability in inflow from upslope drainage serving to dilute the outflow concentrations.

The "input" concentrations (C_i) calculated for Run 1 were lower in all portions compared to values for other runs (Table 3.9), reflecting differences in steady-state concentrations during the four tests (Table 3.8). Small Peclet number (P) ranging from 0.12 to 6.2 (Table 3.9) might indicate larger dispersive transport of solutes relative to convective transport. However, small P values for matrix flows may result from the short "flow" length (L=2.02m) relative to the minimum mixing length (Germann, 1991). Similar problems may arise in the breakthrough analysis for macropores due to effects of lumping macropores into several groups (Ziemer, 1992).

With exception for Run 3, values of V_o (effective pore volume) calculated for the flow-averaged breakthrough data from the entire profile were only slightly different between the three tests despite the different antecedent conditions and application rates (Table 3.9 and Fig. 3.11). Because these tests were conducted in nearly saturated conditions, these results may follow findings of Dyson and White (1989) and Hornberger et al. (1990) that indicated that mixing volumes were less than half of the total volume of pore water. Ratios of V_o (effective pore volume) to total volume of pore water (measured in the field by tensiometers) were 0.36, 0.40, 0.65, and 0.38 for Runs 1 to 4, respectively (Table 3.9). Except for Run 3 again, these ratios are of the same magnitude as values (0.25 to 0.39) reported by

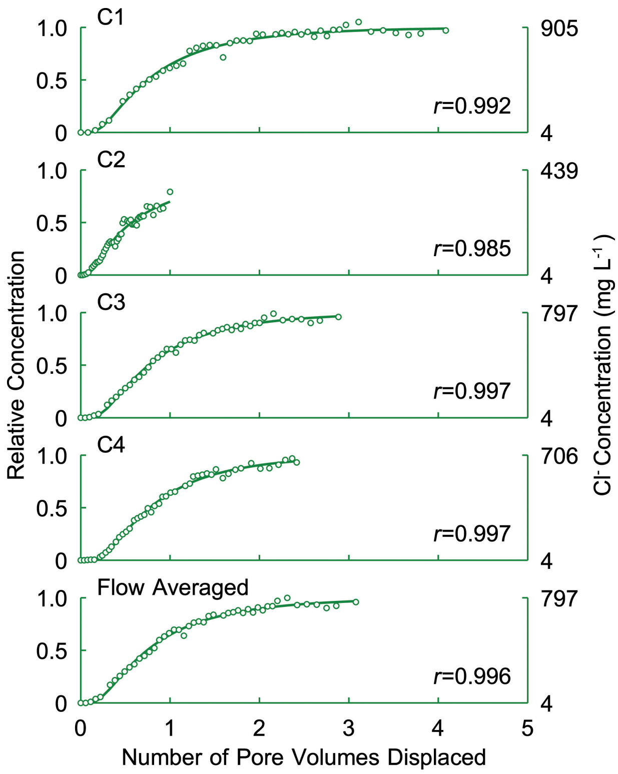

Fig. 3.7 Comparison of experimental (circles) and theoretical (solid lines) chloride breakthrough curves for Run 1 (Tsuboyama et al., 1994b).

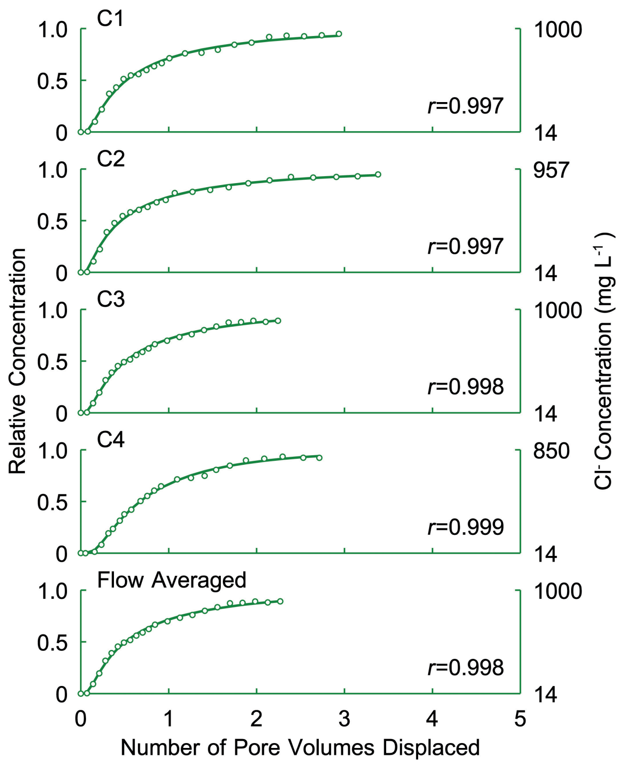

Fig. 3.8 Comparison of experimental (circles) and theoretical (solid lines) chloride breakthrough curves for Run 2(Tsuboyama et al., 1994b).

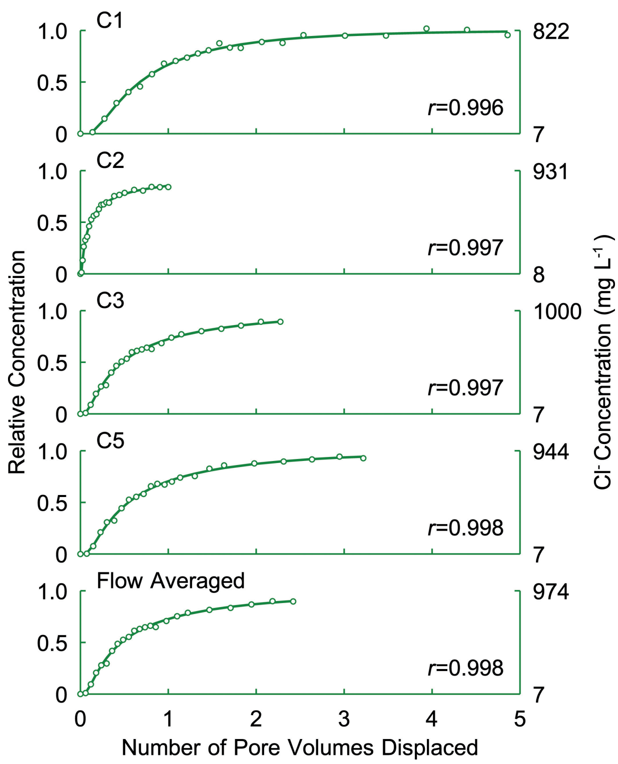

Fig. 3.9 Comparison of experimental (circles) and theoretical (solid lines) chloride breakthrough curves for Run 3.

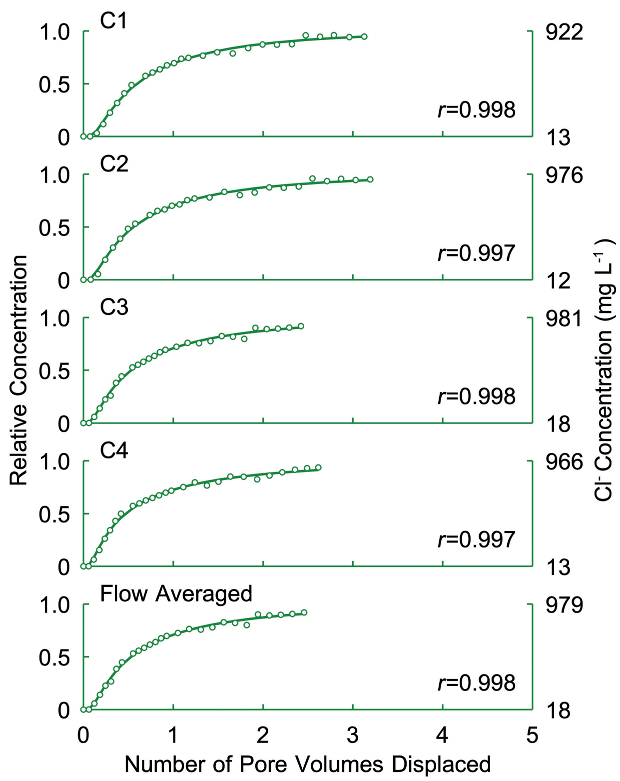

Fig. 3.10 Comparison of experimental (circles) and theoretical (solid lines) chloride breakthrough curves for Run 4.

Table 3.9 Hydrologic properties of various portions of the soil profile derived from the breakthrough analysis

Experiment	Portion	Calculated input concentration mg L^{-1}	Peclet number	Effective pore volume L	Average residence time h	Ratio of pore volume [a] %
Run 1	1	905	2.87	26.76	3.43	6.4
Application rate:	2	439	1.26	25.01	14.00	6.0
60 L h^{-1}	3	797	3.07	113.07	4.86	27.1
(20 mm h^{-1})	4	706	3.29	1.24	5.79	0.3
	Profile	797	2.78	150.55	4.55	36.1
Run 2	1	1000	1.01	4.33	2.72	1.1
Application rate:	2	957	0.79	3.04	2.37	0.7
90 Lh^{-1}	3	1000	0.98	153.87	3.57	37.9
(30 mm h^{-1})	4	850	1.98	0.60	2.95	0.1
	Profile	1000	0.96	163.00	3.53	40.1
Run 3	1	822	2.00	8.08	2.06	2.0
Application rate:	2	931	0.12	66.08	10.00	16.2
90 L s^{-1}	3	1000	0.86	231.83	4.40	56.8
(30 mm h^{-1})	4	727	6.21	0.12	1.54	0.0
	5	944	1.14	1.51	3.11	0.4
	Profile	974	0.82	263.77	4.13	64.7
Run 4	1	922	1.40	2.55	3.12	0.6
Application rate:	2	976	1.19	3.49	3.05	0.8
60 L h^{-1}	3	981	1.06	150.49	4.03	35.4
(20 mm h^{-1})	4	966	0.84	4.89	3.73	1.2
	Profile	979	1.06	161.34	3.97	38.0

[a] Ratio of pore volume to the volume of pore water

Hornberger et al. (1990), although their calculation was based on a transfer function model. Because V_o is an operationally calculated parameter, it should not be directly associated with specific volume of water within the soil. However, much smaller values of V_o relative to total volume of pore water suggest that during these tests preferential flow significantly contributed to transport of tracer within the soil.

An important finding from these tests concerns the variability in effective pore volumes among individual portions of the soil (Fig. 3.12). For the mineral soil matrix (C3), effective pore volume (V_o) varied from 113 to 163 L (Table 3.9, except for somewhat erratic results from Run 3), which is smaller variation relative to difference of application rates (60 to 90 L h^{-1}). In contrast, values of V_o for other portions (C1, C2, and C4) varied much wider (2.6 to 27, 3.0 to 25, and 0.6 to 4.9, respectively, again except for Run 3). Differences in V_o for individual portions of the profile between the tests are as large as 10 times for C1, 8.3 times for C2, and 8.3 times for C4.

Variations in average outflow rate from C1 during tracer application was as large as 10 times (0.81 to 7.8) among three tests (Runs 1, 2, and 4), while those for C2 and C4 were as large as 1.6 fold (1.1 to 1.8) and 6.5 fold (0.20 to 1.3), respectively (Table 3.8). Given that a higher outflow rate during tracer application might result in larger effective pore volume (because of unsaturated conditions), the greatest differences in V_o among runs seem to be in C2 and C4.

These data suggest that effective pore volumes of macropores (C2 and C4) and organic-rich soil layer including macropores (C1) are relatively more variable than mineral soil matrix (C3), while the absolute difference in V_o between the tests was largest in C3. Conceptually, an increase in V_o of C1, C2, or C4 may reflect an expansion of surrounding soil (containing mesopores) that interacts with water in macropores (Fig. 3.13). This increase in V_o may also represent the upslope extension of macropore network as illustrated in Fig. 3.13. This latter mechanism would be more important if macropores receive substantial inflow from upslope as supposed to have occurred in C2 in Run 1. Based on the concept illustrated in Fig. 3.13, increases in V_o of macropores would reduce V_o of the soil matrix. If matrix flow was influenced by preferential flow, the soil matrix would have the similar properties related to solute transport as macropores, and the changes in V_o of macropores and the soil matrix might offset each other. Then, V_o of the entire soil block might not change apparently. This seems to be the case in these experiments. Although the flow mechanisms proposed in Fig. 3.13 are conceptual, the supporting data clearly show: (1) the importance of variable contributions from the different portions of the profile and (2) the interactions of the soil matrix and macropores to the transport of water and solute within the soil.

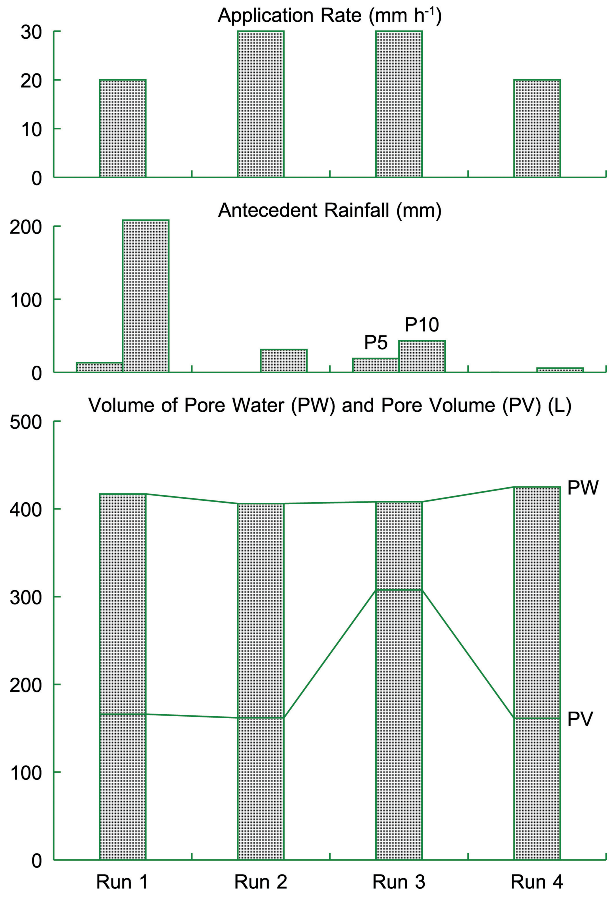

Fig. 3.11 Comparison of volume of pore water and pore-volume calculated from breakthrough curves for the entire soil profile.

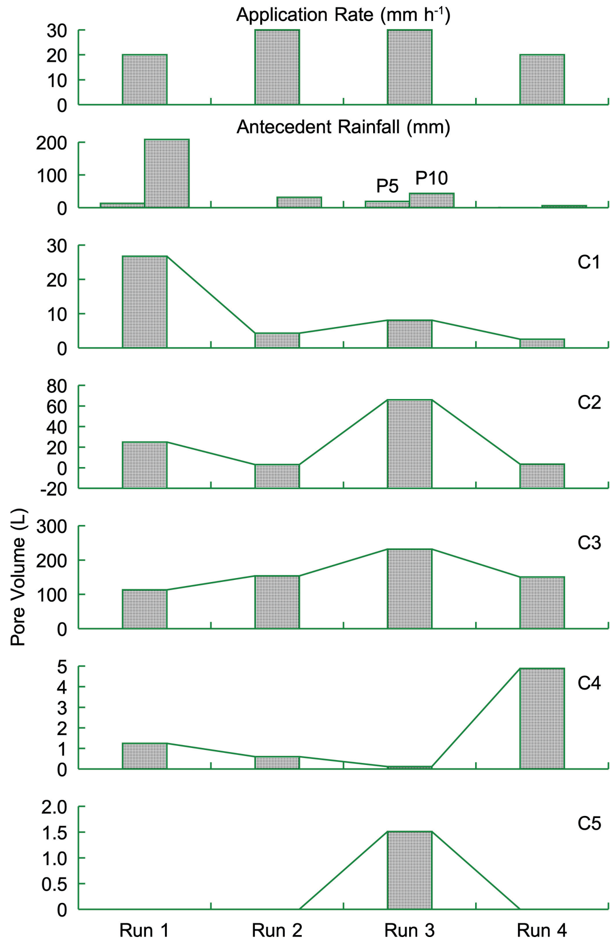

Fig. 3.12 Comparison of pore values calculated from breakthrough curves for each compartment of the soil profile.

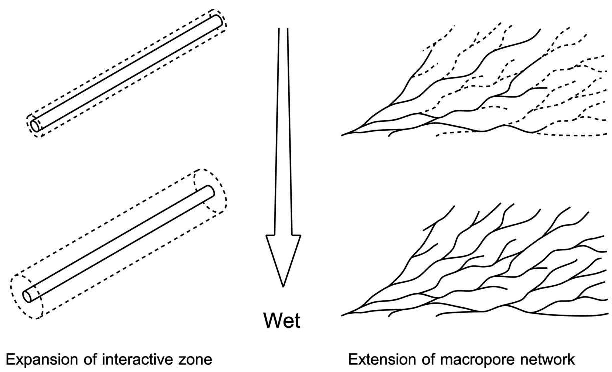

Fig. 3.13 A conceptual illustration of an expansion of surrounding soil that interacts with water in macropores and the extension of macropore network upslope (Tsuboyama et al., 1994b).

3.8.Conclusion

Subsurface flow from various portions of a steep, forest soil profile was evaluated by four sets of step-change miscible displacement tests at different application rates and for antecedent hydrological conditions. Subsurface flow and tracer breakthrough from five portions of the soil profile (the organic-rich soil layer including macropores, the mineral soil matrix, and three groups of macropores in the mineral soil layer) were individually measured and analyzed using a convective-dispersive model. Despite the different application rates, there was little difference in average outflow rates from macropores in the mineral soil among the tests, yet for matrix flows there were detectable differences. In these tests, outflow from mineral horizon macropores, especially for very wet hydrological conditions, had consistently lower Cl^- concentrations than matrix flow, suggesting flow contribution from upslope serving to dilute the outflow concentrations. Effective pore volume (V_o) calculated for the flow-averaged breakthrough data from the entire profile was much less (< 40 %) than the estimates of total volume of pore water, suggesting that preferential flow significantly contributed to subsurface transport of tracer. The effective pore volume for the entire profile increased only slightly with increasing application rate; however, the relative proportions of pore volumes calculated for individual portions varied considerably. These variations are attributed to different upslope drainage conditions, and not to differences in hydraulic loading. Although data presented in this paper do not directly elucidate specific mechanisms of solute transport in the soil matrix and macropores, they clearly show the variability in relative contributions and interactions of the soil matrix and macropores to the transport of water and solute within the soil. Knowledge on such dynamic nature of various flow paths in the soil would improve our understanding (alternatively, our perceptual model) of subsurface hydrology.

4 Hollow to catchment scale variabilities

4.1 Introduction

Topography of headwater areas is generally characterized with geomorphic hollows located in the middle to upper portions of the hillslopes. These hollows are known to be sites of active geomorphic processes (e.g., Sidle et al., 1985) as well as potential source areas of runoff (e.g., Tsukamoto and Ohta, 1988) and solute transport (e.g., Luxmoore et al., 1990). Such hollows are alternatively called zero-order basins since they are located in the uppermost portions of 1st-order basins (Tsukamoto et al., 1982). By definition, zero-order basins have no channels and drain only sporadically. Consequently their role in catchment hydrology may be overlooked in watershed experiments where hydrometric measurements are conducted at the sites where water flows continuously. Sidle et al. (1995) demonstrated that a hollow with shallow soils contributed similar magnitudes of storm flow (per unit area) as subsurface hillslope drainage after a threshold of saturation was reached. Such significant contributions suggest the need for further research on quantitative evaluation of zero-order basins as potential source areas for runoff generation in higher-order basins.

Recently many detailed hydrometric and geochemical investigations have been conducted for relatively planar hillslopes (e.g., Brammer and McDonnell, 1996; McDonnell et al., 1998) as well as for geomorphic hollows (e.g., Buttle and Peters, 1997; Anderson et al., 1997). These studies have advanced our conceptual understanding of specific pathways of subsurface flow as well as their relative contributions to runoff from the specific topographic unit (i.e., a hillslope segment or a hollow) during natural and artificial storms. However, relevance of each pathway and/or topographic unit to catchment hydrology remains in question. For instance, the timing, frequency, and magnitudes of hydrological response of such topographic units would be essential information not only for predicting streamflow generation but also for assessing transport of sediment and/or solutes from headwater drainages over long periods.

As such, this chapter aims to evaluate the relative contribution of a zero-order basin to discharge from a 1st-order catchment as well as to elucidate internal factors affecting its hydrological response. Specifically results from simultaneous measurements of runoff, piezometric heads, and soil temperatures in the hollow over the course of a year are presented and discussed.

4.2 Site description

The study presented in this chapter was conducted at the 2.48 ha 1st-order catchment called Forest Basin B (hereafter, referred to as HB) in the Hitachi Ohta Experimental Watershed (Fig. 2.1). HB includes two gauged subcatchments called Forest Basin A and Zero-Order Basin (hereafter, referred to as HA and HZ, respectively) in its upper portion (Fig. 2.4). HA is a 0.84 ha 1st-order basin comprised of two zero-order basins with relatively gentle slopes (mean gradient: 27°). HZ is a 0.25 ha unchanneled hollow incised deeply with steep sideslopes (mean gradient: 33°). For both HZ and HA, distribution of soil depth to bedrock was measured using knocking pole penetration devices (Tsuboyama et al., 1994a). Soils in these two basins are generally shallower along the axes of the hollows and deeper near the topographic divides (Fig. 2.4). Soil depths in HA ranged from 0.4 to 4.7 m with an average of 2.1 m. Soil depths in HZ ranged from 0.4 to 4.2 m with an average of 1.4 m.

4.3 Field instrumentation

Streamflow was continuously recorded at calibrated 60° V-notch gauging weirs at the outlet of HB and HA (Photo 4.1). Runoff was also measured at a similar installation at the outlet of HZ where discharge was only observed during storm events.

Eight float-type recording piezometers were installed at the soil-bedrock interface (0.5 to 1.2 m depth) along the longitudinal axis of HZ (Fig. 4.1; Photo 4.2). Hereafter, these piezometers are referred to as B1, B2, B3, B4, A1, A2, A3, and A4, respectively, as noted in Fig. 4.1. All piezometer tubes (43 mm inner diameter) were perforated in the lower 10 cm (Fig. 4.2). Water level in the tube was recorded every 30 minutes using a displacement transducer connected to a data logger.

Soil temperature was monitored at the two profiles in the upper portion of the hollow as well as 2 m upslope from the outlet of the hollow (Fig. 4.1). Hereafter, these three locations

Photo. 4.1 A 60° V-notch gauging weir installed at the outlet of HB.

Photo. 4.2 Piezometers located in the head of ZB.

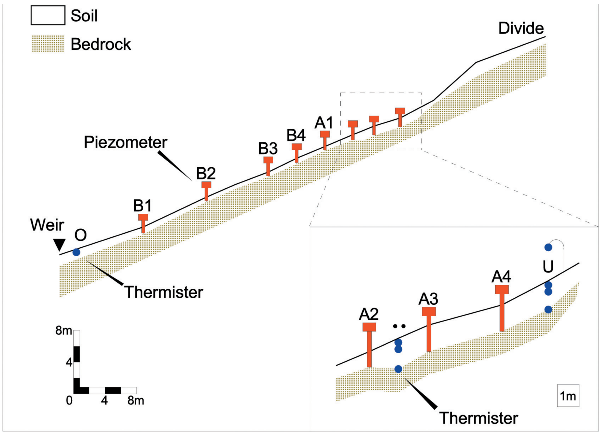

Fig. 4.1 Surface and bedrock topography along the longitudinal axis of the zero-order basin and locations of instruments (Tsuboyama et al., 2000).

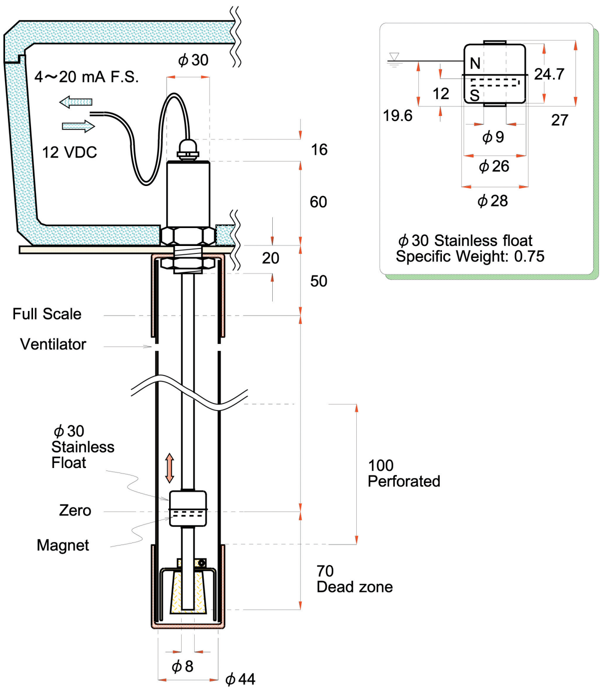

Fig. 4.2 Structure and dimensions of a float-type piezometer.

are referred to as U, L, and O, respectively. The relatively lower profile (L) is located at the center of A2 and A3 piezometers. The upper profile (U) is located 1.2 m upslope (lateral distance) from the uppermost piezometer (A4), above which the slope becomes much steeper up to the topographic divide (Fig. 4.1). In both profiles, thermister probes were installed at the depths of 0.2 and 0.5 m as well as at the soil-bedrock interface (1.4 and 1.3 m deep for L and U, respectively). Soil temperature near the outlet (O) was measured only at the depth of 0.2 m, because of limited availability of instruments. Air temperature was measured at the height of 1.5 m above the surface of the profile U using a similar thermister probe. Temperature data were collected every 30 minutes and calibrated with results from preliminary laboratory tests of the probes against a standard mercury thermometer.

Precipitation was measured using recording and storage raingauges located at the meteorological station (hereafter, referred to as MS; Photo 4-3). MS is an open site on the ridge top located 250 m north of the outlet of HZ (Fig. 2.1). Rainfall records at MS were well correlated with short-term data collected at the canopy interception plot (IC in Fig. 2.1) adjacent to HZ. Thus, rainfall over the small watershed was assumed to be uniform. Also rates of interception and evaporative losses associated with forest cover were assumed to be uniform over the forested area (i.e., HB). Precipitation data at MS were collected every 10 minutes.

4.4.Seasonal variations in runoff

Fig. 4.3 shows seasonal variations in daily precipitation and daily maxima of piezometric heads as well as daily discharges from HZ, HA, and HB from 1992 through 1998. Seasonal patterns of precipitation during these years were similar to those typically observed at the site: two major extended rainy seasons preceded by extended dry periods in late spring and mid-summer (Fig. 2.2). Hereafter, daily amounts of precipitation and discharges from HZ, HA, and HB are referred to as P, Q_z, Q_a, and Q_b, respectively. All of these variables are in mm d^{-1}, i.e.,

Photo. 4.3 Meteorological station.

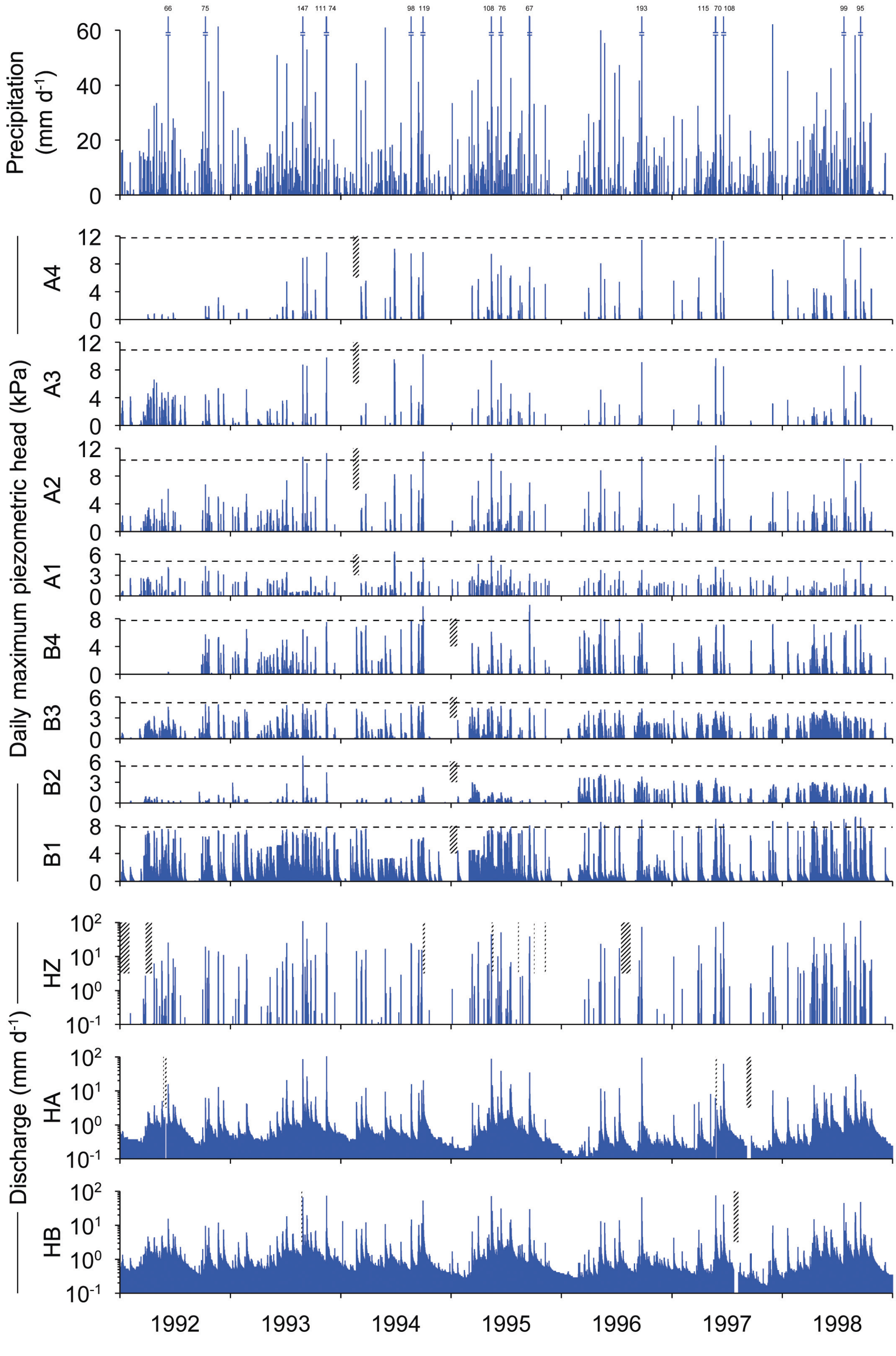

Fig. 4.3 Seasonal variations in daily precipitation, daily maxima of piezometric heads, and daily discharges from the three nested drainages (HZ, HA, and HB in Fig. 2.1) . Hatched areas in piezometric heads and discharge hydrographs indicate that data were missed during that period due to troubles associated with measurement devices. Horizontal broken lines in the graphs of piezometric heads represent thresholds of artesian conditions.

on a unit area and daily basis.

While both HB and HA maintained continuous streamflow runoff from HA was less than from HB for dry conditions (Fig. 4.3). This trend is more evident in Fig. 4.4, where both Q_a and Q_z are plotted against Q_b. For values of Q_b<5 mm d^{-1}, Q_a was consistently smaller than Q_b. Moreover, ratios of Q_a to Q_b generally became smaller with increasing P for this range of Q_b (Fig. 4.4). This convergence is due to the fact that Q_a did not increase to the extent as Q_b during rainstorms with relatively dry conditions (Sidle et al., 1995).

In contrast to sustainable discharges from HA and HB, runoff from HZ was sporadic (Fig. 4.3). Runoff from HZ was negligible (<0.001 mm d^{-1}) for Q_b<0.5 mm d^{-1}. For wetter conditions above this threshold, HZ augmented stormflow. Ratios of Q_z to Q_b increased rapidly from zero up to unity with increasing P and/or Q_b (Fig. 4.4).

Large daily discharge from HB (Q_b>5 mm d^{-1}) generally occurred on days when precipitation (or short-term antecedent precipitation) exceeded 50 mm d^{-1} (Fig. 4.3). Even during a few of these wet conditions some values of Q_z/Q_b were smaller than unity (Fig. 4.4). However, this ratio could be influenced by the "carry over" effect of Q_b from the previous days. Thus, discharges from HB, HA, and HZ were quite similar for these wettest conditions, regardless of their different topographic and geomorphic attributes.

In summary HZ appeared to behave at three different levels as a contributor to runoff generation in HB: (1) no contribution when Q_b<0.5 mm d^{-1}, (2) non-linear contribution when 0.5<Q_b<5 mm d^{-1}, and (3) linear contribution when Q_b>5 mm d^{-1}. These findings are consistent with results from the previous study at the site (Sidle et al., 1995), which showed that HZ became gradually more responsive through the periods of increasing wetness (defined by antecedent precipitation) over two months.

4.5 Topographic controls

As reported in many studies (e.g., Dunne and Black, 1970; Anderson and Burt, 1977; Tanaka, 1982; Sidle, 1984; Tsuboyama et al., 1994a), shallow groundwater or piezometric response at a point scale reflects combined effects of many factors. These factors include prestorm and intrastorm characteristics of precipitation as well as topographic and geomorphic attributes of the site such as slope positions, slope gradients, depths to impeding layers, and soil properties associated with subsurface flow. As a result of wide temporal

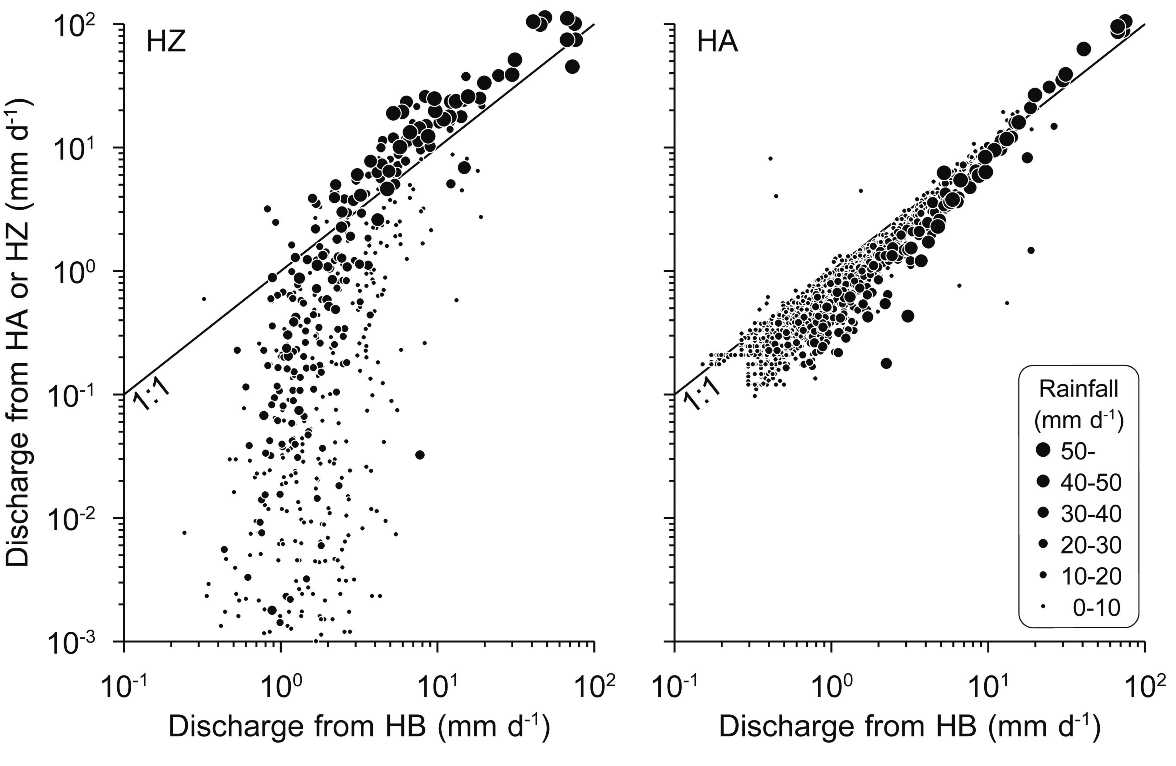

Fig. 4.4 Relationships of daily discharges from HA or HZ to daily discharge from HB from 1992 through 1998. Size of each circle reflects a daily amount of precipitation.

and spatial variations in these conditions, it may sometimes be difficult to clearly delineate effects of each factor on piezometric response from rainfall-response relationships. For these reasons we analyzed piezometric data in relation to runoff from HZ instead of precipitation.

The effect of slope position on the relationship between Q_z and maximum piezometric rise over a range of Q_z is clearly shown in Fig. 4.5. Maximum piezometric levels at downslope site (B1 to B3) increased with increasing Q_z even for relatively dry conditions (Q_z<0.1 mm d^{-1}). This piezometric increase continued at these three locations for the range of Q_z up to around 0.5 mm d^{-1}, where considerable scatter in the data from the lowermost two piezometers was observed (B1 and B2; Fig. 4.1). Above this threshold, piezometric heads at these three locations increased more gradually with increasing Q_z, suggesting that these piezometers became "hydrologically saturated". Such a condition suggests that the sites are at the maximum piezometric level for given range of hydrological loads or inputs.

In contrast, upslope piezometers (A2 to A4) responded mainly when Q_z>0.5 mm d^{-1} (Fig. 4.5). Response of middle slope piezometers (B4 and A1) seemed to exhibit an intermediate threshold response to Q_z, although considerable data scatter was observed (Fig. 4.5).

Overall, Fig. 4.5 suggests that piezometers responded only in the lower to middle positions of HZ during relatively small stormflow events, while major runoff response from HZ coincided with large piezometric rise near the head hollow. Thresholds of piezometric rise in the upper locations (A2 to A4) fell between 0.5<Q_z<1 mm d^{-1} (Fig. 4.5), which correspond to the transition zone where Q_z/Q_b approaches and exceeds unity (Fig. 4.4).

In addition, it should be noted that except for the greatest piezometric rise when Q_z>10 mm d^{-1}, most piezometers indicated that a portion of the upper soil profile was unsaturated. Thus, the relationships between Q_z and piezometric heads in Fig. 4.5 suggest that shallow groundwater, which developed along the trough of the hollow, facilitated pathways of subsurface stormflow. Furthermore, the interrelationships among Q_b, Q_z, and piezometric heads in Figs. 4.4 and 4.5 suggest that non-linear contribution of HZ to discharge from HB can be attributed to temporal variations in the spatial extent of the shallow groundwater above the trough of the hollow. This hypothesis will be further examined later by looking at intrastorm variations in these hydrological variables as well as soil temperatures.

4.6.Seasonal variations of soil temperatures

In the previous sections, runoff and piezometric response of HZ were analyzed on daily basis to assess the total hydrology of HZ in relation to discharge from HB. In this section, a seasonal variation of soil temperature in HZ is used as a tracer for subsequent analyses of short-term variations in the hydrological variables. Thermal signatures have been widely used to investigate groundwater movement (e.g., Suzuki, 1960; Stallman, 1965) as well as to separate snowmelt hydrographs (e.g., Kobayashi, 1985), where flows were relatively slow or assumed constant. A recent study by Tsuboyama et al. (1998) showed that soil temperatures in the head hollow of HZ could fluctuate even during rainstorms, based on data collected at 30 minutes intervals. While thermal signatures may not be conservative as isotopic and certain chemical tracers, the study by Tsuboyama et al. (1998) suggested possibility of using soil temperature for tracing instantaneous signatures in the subsurface that would not be averaged over a collection time.

Fig. 4.6 shows seasonal variations in daily mean soil temperatures measured at the depths of 0.2, 0.5, and 1.3 m in the head hollow (U) and at the depth of 0.2 m near the outlet (O) in HZ from 1996 through 1998. Hereafter, these positions are noted as U_{20}, U_{50}, and U_{130} in reference to their depth in cm in the upper profile U.

At each depth daily mean temperature exhibited nearly sinusoidal seasonal variation, which overlies short-term fluctuations; magnitudes and phases are generally more damped and delayed, respectively, with increasing depth (Fig.4.6). Consequently soil temperature is generally higher near the surface during the summer (June to September) and higher at depth during the winter (November to March). Between these two extremes transition periods occurred around April and October, during which time the vertical distribution of soil temperature became relatively uniform. During such conditions soil temperature may be less useful as a tracer (Tsuboyama et al., 1998).

While not shown as a figure, similar seasonal patterns also appeared in the lower profile (L). Lateral variations in soil temperature between these two profiles (L and U) were very small compared to vertical thermal variations. For the period shown in Fig. 4.6, absolute differences between daily mean soil temperatures at U_{20} and U_{50} averaged 1.1 °C, while at all depths (20, 50 cm, and the soil-bedrock interface) absolute differences between two locations averaged 0.3 °C.

Soil temperature at O_{20} exhibited somewhat different seasonal responses compared to other sites. The responses were nearly identical to soil temperature at U_{50} during relatively wet seasons (June to September) while they became closer to soil temperature at U_{20} during drier seasons (November to March). Lower temperature at O_{20} relative to U_{20} during wet seasons may reflect combined effects of upward saturated-unsaturated flow and higher rates of evaporation due to wetter soil moisture conditions near the outlet.

4.7 Intrastorm response

Hydrological and thermal response in HZ during rainstorms is analyzed in the following sections. Three storm events are examined to accommodate wide variations in hydrological response of HZ (Table 4.1; Figs. 4.7 to 4.9). Major differences among these three events are in storm precipitation (Table 4.1). While not shown in the final three figures, air temperatures at MS and U were consistently higher than soil temperatures during these storms. Thus, temperature of rainwater was

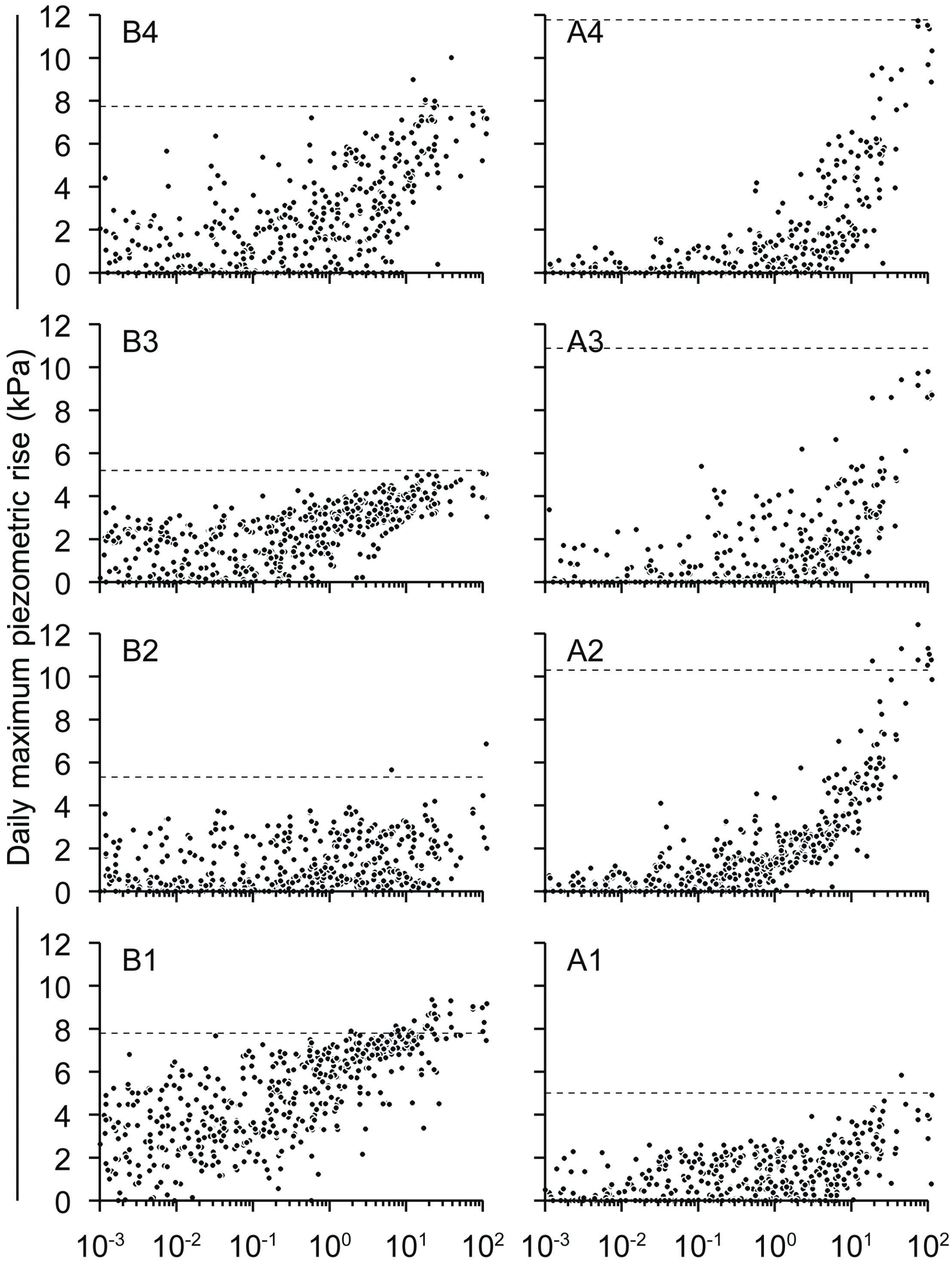

Fig. 4.5 Relationships between runoff from HZ and daily maxima of piezometric heads. Horizontal broken lines represent thresholds of artesian conditions.

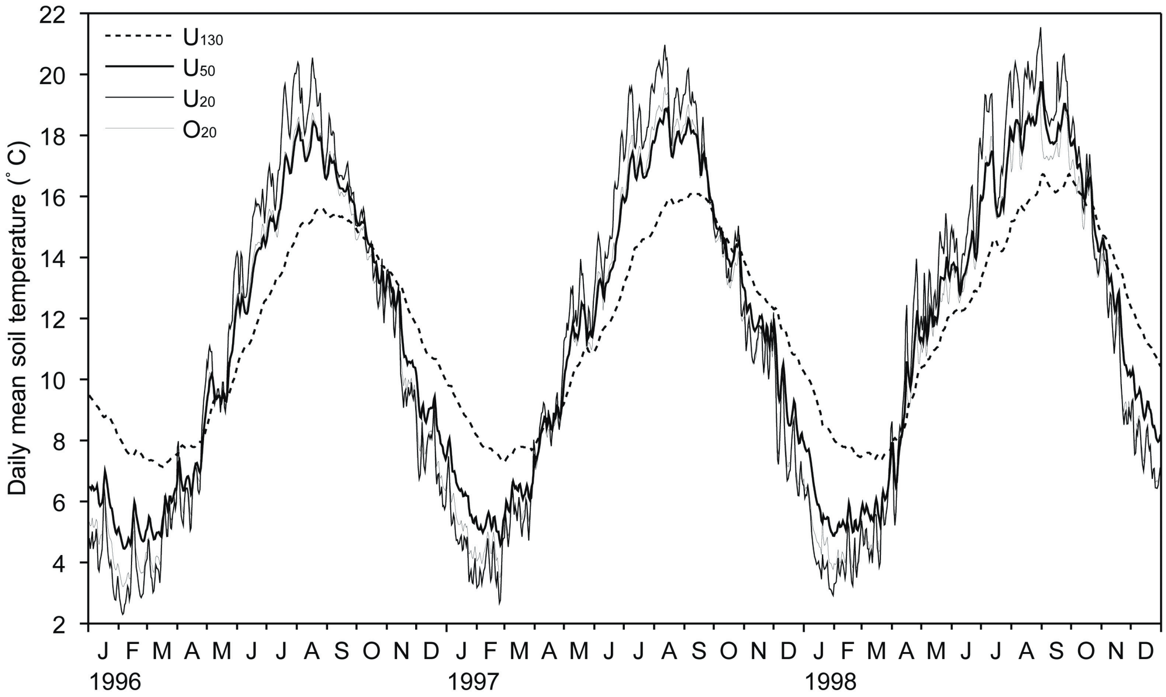

Fig. 4.6 Seasonal variations in daily mean soil temperatures.

assumed higher than soil temperatures although it may be somewhat lower than air temperature as supposed for temperature of a wet-bulb thermometer.

4.7.1 A small storm

Fig. 4.7 shows response of soil temperatures and piezometric heads in HZ as well as runoff from HZ and HB during the relatively small storm on May 2 to 3 in 1996. Values of P, Q_b, and Q_z for the first day (May 2nd) are 15.6, 0.85, and 0.042 mm d^{-1}, respectively, while for the 2nd day (May 3rd) these values are 2.5, 0.78, and 0.001 mm d^{-1}, respectively. Much smaller Q_b and Q_z than P, as well as small Q_z/Q_b ratio, reflect dry antecedent conditions and relatively small amount of storm precipitation (Table 4.1).

During this storm only lower to middle piezometers (B1 to A2) responded (Fig. 4.7). Piezometric rise was generally higher and lasted longer at lower piezometers, suggesting that a wedge of shallow groundwater developed along the lower portion of the trough. Such a wedge shaped groundwater response during dry conditions has been noted at this and other sites (Sidle, 1984; Sidle and Tsuboyama, 1992; Tsuboyama et al., 1994a). During the peak of the rainstorm (1600h to 2000h on May 2nd) soil temperature at O_{20} increased rapidly (Fig. 4.7). Soil temperatures at L_{20}, L_{50}, U_{20}, and U_{50} increased only gradually over the two days, while temperature at the soil-bedrock interface (L_{138} and U_{130}) appeared nearly constant at this time scale (Fig. 4.7). After the peak of rainfall, soil temperature at O_{20} decreased until it approached the soil temperature at U_{50} (Fig. 4.7). As noted in the previous section, soil temperature at O_{20} was rather close to that at U_{50} during this portion of the year (Fig. 4.6).

Assuming that temperature of rainwater was higher than soil temperatures, the rapid thermal increase at O_{20} probably resulted from percolation of rainwater. Effects of percolation on soil temperature may dissipate in the upper profiles (L and U) due to relatively dry moisture conditions. The decline in soil temperature at O_{20} indicates an alteration of the dominant flow direction at O_{20} (i.e., from downward to upward or lateral).

Table 4.1 Rainfall characteristics for three storms during 1996-1997 in Hitachi Ohta, Japan (after Tsuboyama et al., 2000).

Storm date	Storm length	10-days antecedent precipitation	Storm precipitation	Maximum 30-min intensity
	h	mm	mm	mm h^{-1}
May 2, 96	13.5	11.8	18.0	5.4
May 22, 96	10.0	7.0	55.4	37.0
Jun 19, 97	19.5	63.9	108.3	21.4

Although the delayed piezometric response at B1 is somewhat puzzling, this interpretation would explain the timing of runoff from HZ, which was delayed from rapid piezometric rise that occurred at most of the other lower slope sites (Fig. 4.7).

4.7.2 A large storm

Fig. 4.8 shows response of soil temperatures and piezometric heads in HZ as well as runoff from HZ and HB during the relatively large rainstorm on May 22 to 23 in 1996. Total storm precipitation was three-times larger than the May

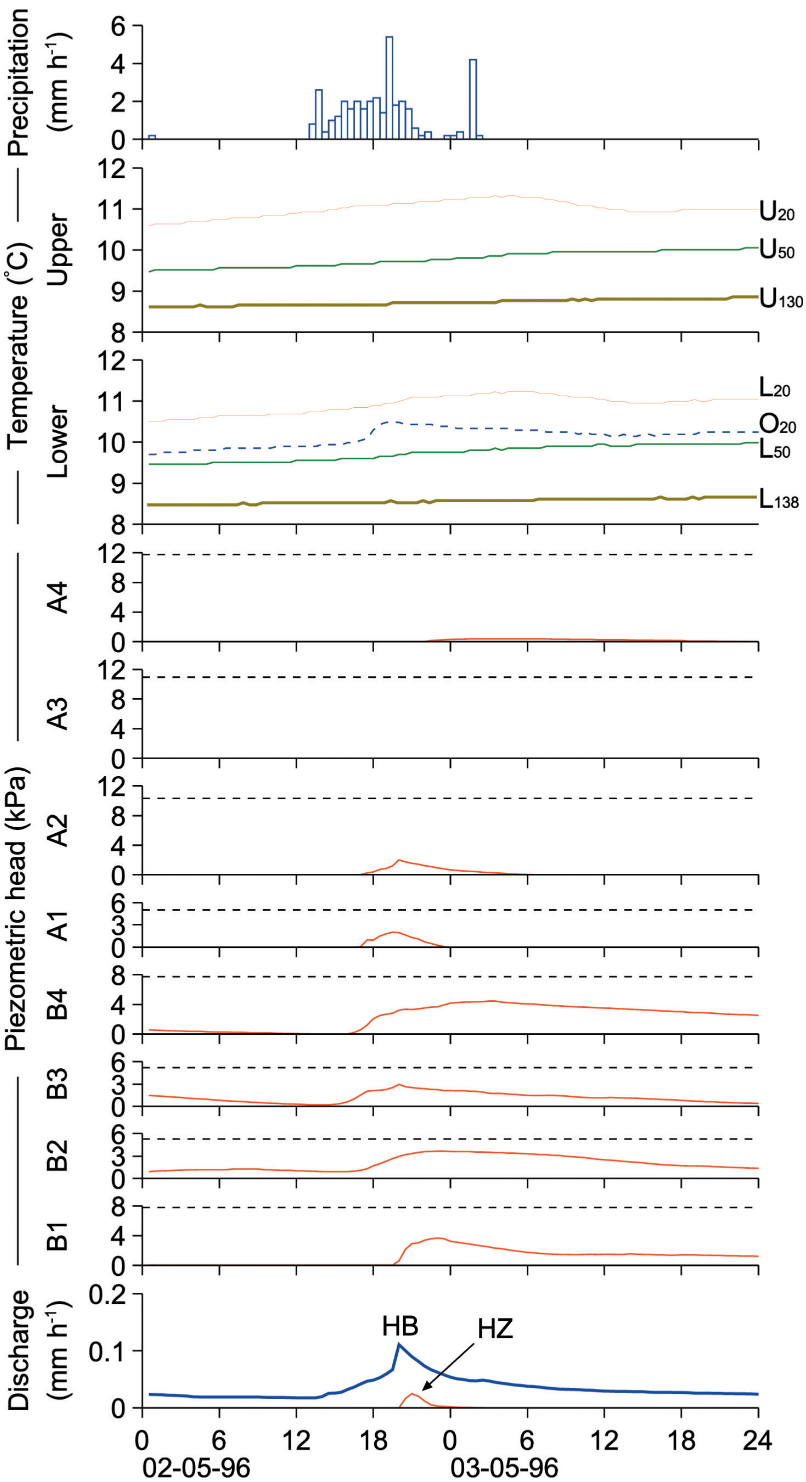

Fig. 4.7 Hydrological and thermal responses in HZ to a small rainstorm. Horizontal broken lines in the graphs of piezometric heads represent thresholds of artesian conditions (Tsuboyama et al., 2000).

2nd storm (Table 4.I). Values of P, Q_b, and Q_z for the first day (May 22) are 55.4, 11.9, and 17.8 mm d^{-1}, respectively, while for the 2nd day (May 23) these values are 0.1, 5.8, and 1.7 mm d^{-1}, respectively. Over the two days, HZ discharged slightly more water than HB, although the difference was very small.

The rainstorm commenced with high intensity burst of rainfall and all piezometers responded almost simultaneously (Fig. 4.8). Piezometric rise lasted longer at lower positions (B1 to B3) while it recessed faster at upper positions (A1 to A4). Such findings have been reported both at this and other study sites (Sidle, 1984; Sidle and Tsuboyama, 1992; Tsuboyama et al., 1994a).

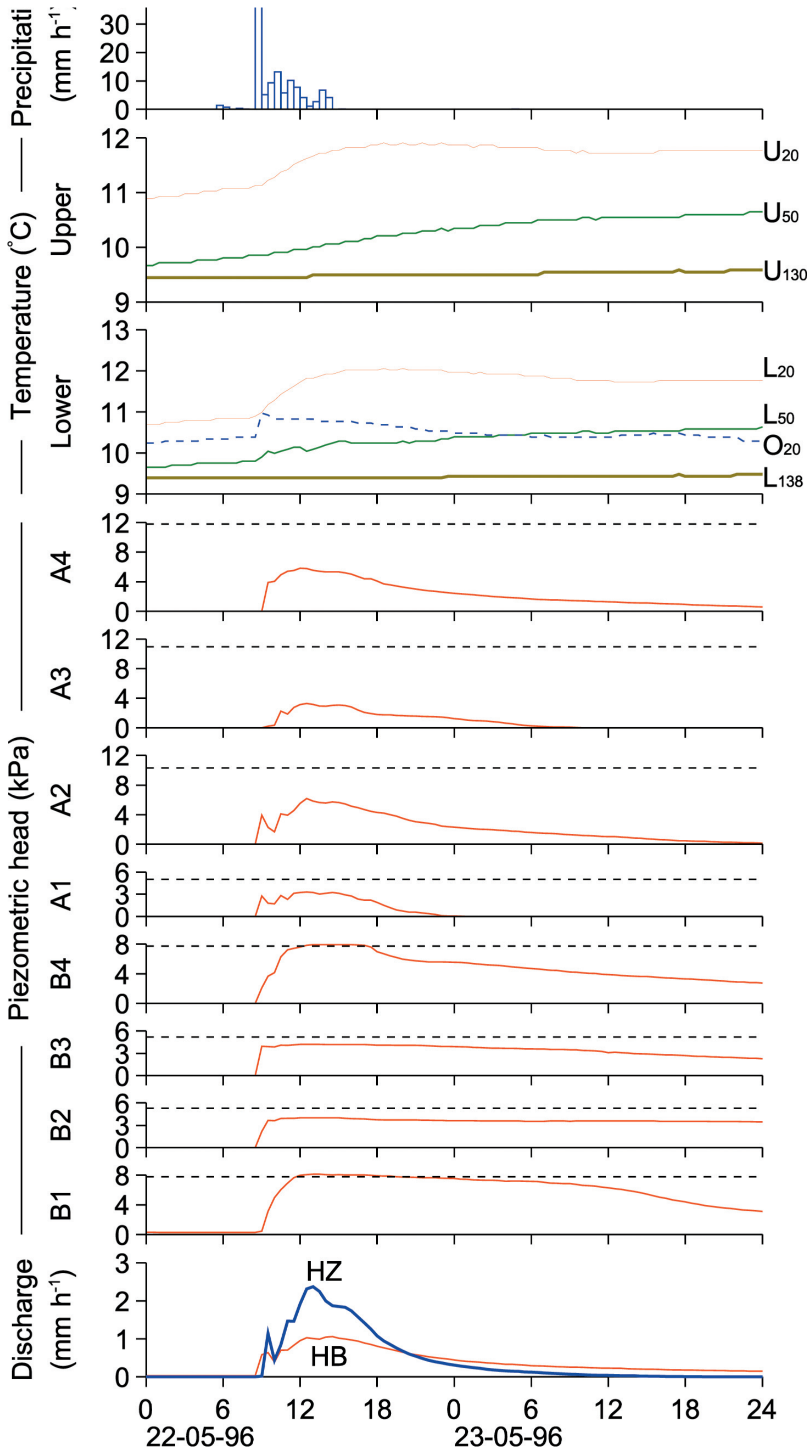

Fig.4.8 Hydrological and thermal responses in HZ to a large rainstorm. Horizontal broken lines in the graphs of piezometric heads represent thresholds of artesian conditions (Tsuboyama et al., 2000).

At the onset of the rainstorm, soil temperature at O_{20} increased rapidly. Soil temperatures at L_{20} and U_{20} also increased, but at a more gradual rate. Thermal response to the rainstorm was not evident for soil temperature at U_{50}, while soil temperature at L_{50} exhibited subtle oscillations overlying the general trend of a gradual increase. Such oscillations may have reflected interactions between rainwater and shallow groundwater, which appeared and disappeared around L_{50} (Tsuboyama et al., 1998). Soil temperatures at L_{138} and U_{130} did not change over two days.

Thermal increases at O_{20}, L_{20}, and U_{20} starting at the onset of the storm were attributed to percolation of rainwater. A much faster thermal rise at O_{20} compared to L_{20} and U_{20} suggest that rapid lateral flow originated from and moved through the relatively shallower subsurface in the lower to middle portions of the hollow. This lateral flow also comprised the initial peak that preceded the major runoff response from HZ (Fig. 4.8).

After the rapid initial rise, soil temperature at O_{20} gradually decreased until stormflow from HZ ceased. Notably soil temperature at O_{20} decreased to levels lower than soil temperature at U_{50}, thus contrasting the trend observed during the May 2nd storm event (Fig. 4.7). It suggests that at least the later portion of runoff from HZ during this rainstorm was comprised of subsurface stormflow originated from and/or moved through the relatively deeper subsurface in the upper portion of the hollow.

4.7.3 A very large storm

Fig. 4.9 shows response of soil temperatures and piezometric heads as well as runoff from HZ and HB to the very large rainstorm during June 20-21 in 1997. Although data from 1997 were not analyzed in the previous sections, this storm event is presented as an example of rapid thermal fluctuations during a rainstorm. Values of P, Q_b, and Q_z for the first day (Jun 20) are 108.2, 40.8, and 104.5 mm d^{-1}, respectively, while for the 2nd day (June 21) these values are 0, 12.5, and 8.76 mm d^{-1}, respectively. The very large runoff from HZ, which exceeded precipitation during the two days, may have been overestimated because of sedimentation at the gauging weir that was observed after the event.

For this particularly large storm, the upper three piezometers (A2, A3, and A4) responded almost identically; at A2, artesian conditions appeared and lasted for several hours. Although runoff response from HZ may have been overestimated, it corresponded to piezometric response at these locations.

Soil temperature at O_{20} did not change rapidly during the storm, in contrast to rapid increases observed in two May 1996 storms (Figs. 4.6 and 4.7). This slow thermal response may be attributed to the groundwater that persisted from the previous storm in the lower portion of the hollow (Fig. 4.9). Such wet conditions would dissipate the thermal effects of rainwater by directly impeding infiltration of rainwater (i.e., causing saturation-excess overland flow) and by facilitating transport of water from upslope, which temperature could be relatively stable as a result of active thermal mixing in the upper portion of the hollow as described below. Soil temperatures in the upper profile (L and U) fluctuated considerably even while soil temperatures at the soil-bedrock interface (L_{138} and U_{130}) remained constant during this active piezometric response. Soil temperature at L_{50} started to increase at the onset of the major part of the rainstorm. Thermal increase at L_{50} continued until the initial rapid piezometric rise at the two sites (A2 and A3) adjacent to profile L (Fig. 4.9). Later, soil temperature at L_{50} repeated a similar increase-decrease pattern for the next peak of piezometric response at A2 and A3 (Fig. 4.9). Thermal fluctuations at L_{20}, U_{20}, and U_{50} were gentler but still showed similar responses - i.e., decreases in temperature began when the groundwater surface (as measured in piezometers) exceeded the depths of the thermisters.

This thermal response clearly indicates that the large piezometric rise at these locations (A2, A3, and A4) was caused not only by infiltrating rainwater but also by accumulation of relatively cold water, most likely coming from further upslope of the head hollow through convergent subsurface flow. Such contribution was less evident during the relatively small storm on May 2, 1996 (Fig. 4.7), possibly because of drier moisture conditions in the upper portion of HZ.

Thus, by analyzing three rainstorms with different magnitudes, the runoff contributions of HZ were found to vary widely due to cumulative effects of the following successive hydrological processes: 1) variations in soil moisture conditions in and around the head hollow, as a control on convergent subsurface flow, 2) generation of convergent subsurface flow in the head hollow, as a control on spatial extent of the groundwater above the trough, and 3) temporal and spatial variability of the groundwater which appears above the trough of the hollow, as a control on subsurface source areas as well as pathway of subsurface stormflow. Further investigations are needed related to soil moisture conditions in the upper portion of HZ as well as contributions of sideslopes located in the lower portion of HZ.

4.8 Conclusion

As a result of runoff measurements during the course of a year, HZ appeared to contribute to runoff generation in HB at three levels: (1) no contribution (Q_z/Q_b=0 regardless of P or Q_b) for Q_b<0.5 mm d^{-1}, (2) non-linear contribution (0<Q_z/Q_b<1 depending on Q_b and P) for 0.5<Q_b<5 mm d^{-1}, and (3) linear contribution (Q_z/Q_b=1 regardless of P or Q_b) for Q_b>5 mm d^{-1}. Piezometric data suggested that spatial extent of the groundwater along the trough affected runoff response of HZ. Specifically major contribution of HZ to discharge from HB generally coincided with large piezometric rise near the head hollow. Soil temperatures in the head hollow fluctuated even during some large rainstorms, indicating that such large piezometric rises were caused by contribution from further upslope via convergent subsurface flow. Thus, shallow groundwater, which would develop above the trough

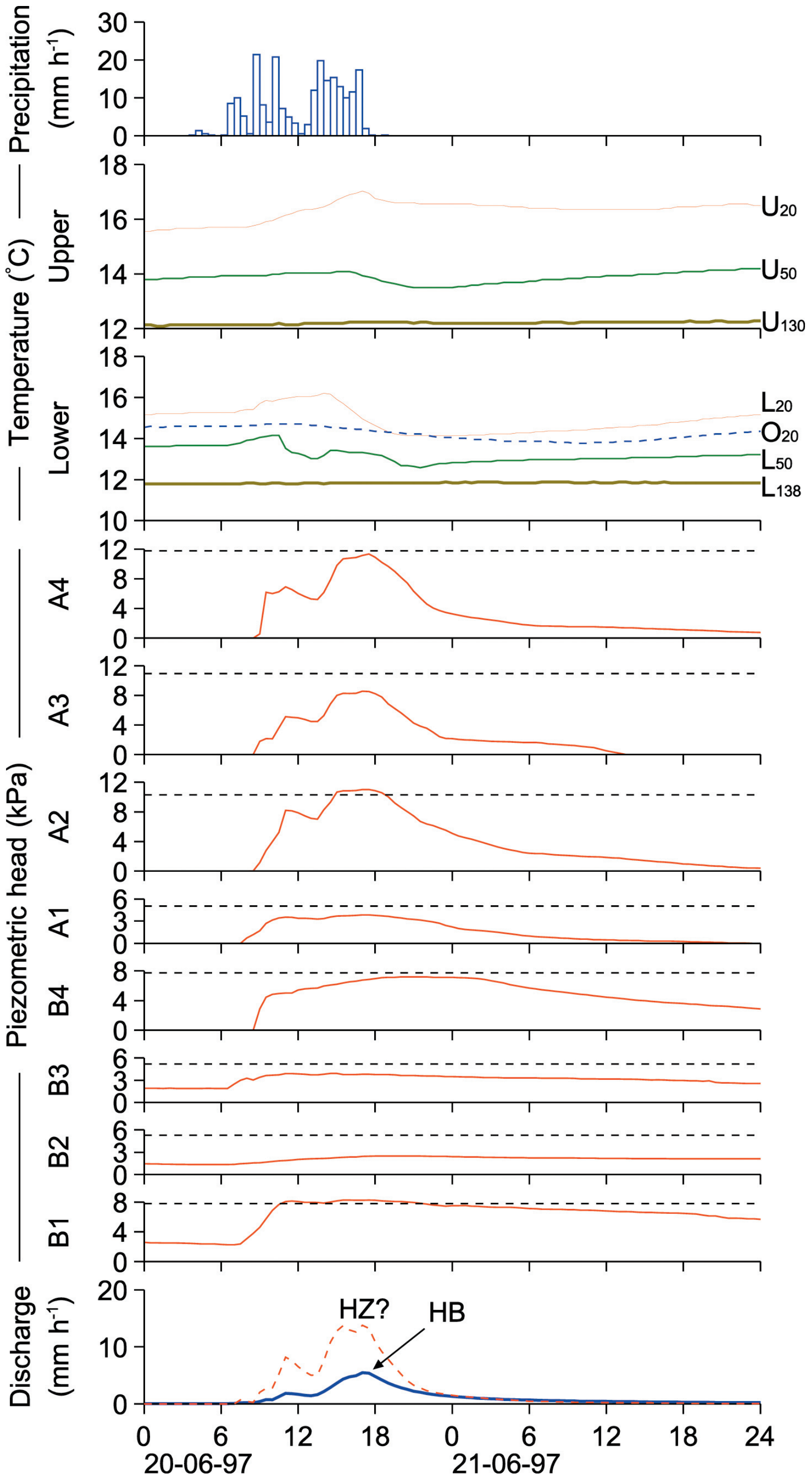

Fig. 4.9 Hydrological and thermal responses in HZ to a very large storm. Horizontal broken lines in the graphs of piezometric heads represent thresholds of artesian conditions. Runoff from HZ during this storm may be overestimated because of sedimentation at the gauging weir that was observed after the event (Tsuboyama et al., 2000).

of HZ, would not always extend from the base to upslope but may appear simultaneously near the head hollow due to a contribution of convergent flow. This additional contribution related to upslope topography may create further variable and non-linear hydrological response in HZ relative to planar hillslopes. While thresholds proposed in this study may differ from site to site, these findings help us in determining the timing, frequency, and magnitudes of hydrological response of zero-order basins as potential source areas of stormflow in larger catchments over long periods.

5 Summary

This study examined temporal and spatial variability of subsurface flow paths and sources of streamflow in a small forested catchment.

In the first part (chapter 3), subsurface flow from various portions of a soil profile on a steep, forested hillslope was evaluated by four sets of step-change miscible displacement tests at different application rates and for various antecedent hydrological conditions. Solutions of NaCl (1000 mg L^{-1} Cl^-) were applied at steady-state rates (equivalent to 20 and 30 mm h^{-1} of standing water over the entire plot area) using a line irrigation source located 1.5 m upslope (lateral distance) from an excavated soil pit. Subsurface flow and tracer breakthrough from five portions (the organic-rich soil layer including macropores, the mineral soil matrix, and three groups of macropores in the mineral soil layer) of the soil profile were individually measured and analyzed using a convective-dispersive model. Matrix flow dominated discharge from the soil pit during tracer tests (70-93 % of total discharge). However, during wet periods with upslope drainage, macropores (including organic-rich soil) contributed proportionally more flow than during periods when upslope drainage was minimal. Outflow from macropores during the test with wet antecedent conditions had lower Cl^- concentrations than drainage from the soil matrix, suggesting dilution in macropores from upslope drainage. Effective pore volumes calculated for the flow-averaged breakthrough data from the entire profile were much less (< 40 %) than the estimates (measured by tensiometers) of total volume of pore water, suggesting that preferential flow significantly contributed to subsurface transport of tracer. The pore volume for the entire profile increased only slightly with increasing application rate; however, the relative proportions of pore volumes calculated for individual portions varied proportionally to antecedent hydrological conditions. These changes are attributed to the expansion of individual macropores with surrounding soil and the lateral extension of macropore networks during wetter conditions.

In the second part (chapter 4), roles of a zero-order basin in catchment hydrology and its internal hydrological processes were investigated. Runoff, piezometric heads, and soil temperatures were measured for a 0.25 ha zero-order basin (HZ) together with discharges from an adjacent 0.84 ha 1st-order basin (HA) and a larger 2.48 ha 1st-order basin (HB) which includes both HZ and HA. Data collected over a year showed HZ contributed to runoff generation in HB at three different levels. While continuous runoff was recorded from both HB and HA, no substantial runoff was measured for HZ during dry conditions when discharge from HB<0.5 mm d^{-1} (level 0: no contribution). For wetter conditions above this threshold HZ augmented stormflow and the discharge ratios of HZ to HB (on a unit area basis) increased rapidly from zero up to unity with increasing wetness (level 1: non-linear contribution). During the wettest periods when discharge from HB>5 mm d^{-1} all three basins generated runoff of the same order per unit area (level 2: linear contribution). Piezometers installed above the soil-bedrock interface (0.5 to 1.2 m depth) along the longitudinal axis of HZ responded only in the lower locations when runoff from HZ<discharge from HB. Conversely major runoff contribution from HZ to discharge from HB generally coincided with large piezometric rise near the head hollow. Soil temperatures in the head hollow fluctuated even during some rainstorms, indicating that such large piezometric rise was caused by convergent subsurface flow from further upslope. Thus, shallow groundwater, which developed above the trough of HZ, would not always extend from the base to upslope but may appear simultaneously in the head hollow. This additional contribution due to upslope topography may create additional variability and non-linearity in runoff response from HZ relative to planar hillslopes.

While investigations were conducted at two different scales (i.e., soil to hillslope and a hollow to catchment scales), common features can be seen in the fact that a certain degree of wetness is needed for potential preferential flow pathways such as macropores and hollows to act as actual flow paths. Once this threshold has been reached, each flow pathway would extend its drainage space by hydrologically linking different locations in space, thus increasing its relative contribution to discharge at a larger scale (Sidle et al., 2000; Sidle et al., 2001). This hydrological linkage (and conversely disconnection) which occurs at various scales in the watershed can be seen as a different expression of the variable source area concept. The major achievement in this study is that it associated variations in source areas with potential preferential flow pathways which could operate at various scales and that it revealed processes in which they change their ability as a conduit. Detailed data and analyses will enhance our understanding of water transport processes in mountainous catchments and also be useful in watershed management practices through validation and improvement of distributed hydrological models.

6 Acknowledgements

The author would like to acknowledge Profs. Masakazu Suzuki and Takehiko Ohta for their continuous encouragement and invaluable suggestions to the author in preparing this paper. Appreciation is extended to Profs. Hiroshi Kobayashi, Tsuyoshi Miyazaki, and Hirofumi Shibano, who also gave invaluable comments and suggestion in finalizing this paper. Special appreciation is given to Prof. Isao Yamaguchi for introducing the author to the field of forest hydrology. Also it should be greatly appreciated that Profs. Kunihiko Nishio and Hiroshi Kawabe helped the author in getting into this field when the author was an undergraduate student in the course of forest hydrology.

All the works presented in this paper have been conducted in close conjunction with many colleagues in and out of the Forestry and Forest Products Research Institute, Japan. Collaboration of Drs. Roy C. Sidle, Shoji Noguchi and Ikuhiro Hosoda with the author over many years should be greatly acknowledged. A special note of gratitude is given to Drs. Toshio Shimizu, Motohisa Fujieda, Akio Kikuya, Mayumi Ogawa, and Kinuyo Ushiro for their helps in conducting field investigations and indoor analyses as well as many suggestions throughout the author's works. Many thanks to Drs. Hirotaka Ochiai, Toshiaki Sammori, Yoshikazu Ohtani, Takeshi Morisawa, Katsumi Yamanoi, and Yasuko Mizoguchi for their support in preparation of the tracer experiments.

Soil depth data for the experimental site were partly collected during the Earth Watch campaign in 1994, entitled "Beneath Japan Cedar Forest". Special appreciation is given to Dr. Jeff McDonnell, the principal investigator in this field campaign, as well as to the Earth Watch volunteers. Contributions from Drs. Akira Shimizu, Shigeki Murakami, Toshio Abe, Tayoko Kubota, Naoki Kabeya, and Jian-jun Zhang in recent soil survey are also appreciated.

This study was partly catalyzed and funded by a Science and Technology Agency Fellowship of Japan (#190056), which was awarded to Dr. Roy C. Sidle in 1991. The author thanks Prof. Makoto Tani for promoting this cooperative research and valuable suggestion. A special note of gratitude should be given to anonymous refrees on this manuscript. Last but not least, the author would like to say thanks to the family.

7 References

Anderson, M.G. and Burt, T.P. (1977) Automatic monitoring of soil moisture conditions in a hillslope spur and hollow, J. Hydrol., **33**, 27-36.

Anderson, M.G. and Burt, T.P. (1990a) Process studies in hillslope hydrology: an overview, in Anderson, M.G. and Burt, T.P. (eds.), Process studies in hillslope hydrology, John Wiley & Sons, Chichester, UK,1-8.

Anderson, M.G. and Burt, T.P. (1990b) Subsurface flow, in Anderson, M.G. and Burt, T.P. (eds.), Process studies in hillslope hydrology, John Wiley & Sons, Chichester, UK, 365-400.

Anderson, S.P., Dietrich, W.E., Montgomery, D.R., Torres, R., Conrad, M.E. and Loague, K. (1997) Subsurface flow paths in a steep, unchanneled catchment, Water Resour. Res., **33**, 2637-2653.

Atkinson, T.C. (1978) Techniques for measuring subsurface flow on hillslopes, in Kirkby, M.J. (ed.), Hillslope Hydrology, John Wiley & Sons, Chichester, UK, 73-120.

Aubertin, G.M. (1971) Nature and extent of macropores in forest soils and their influence on subsurface water movement, USDA For. Serv. Paper NE-192, p33.

Bathurst, J.C. (1986) Physically based distributed modeling of an upland catchment using the Système Hydrologique Europèan, J. Hydrol., **87**, 79-102.

Bernier, P.Y. (1985) Variable source areas and storm-flow generation: An update of the concept and a simulation effort, J. Hydrol., **79**, 195-213.

Betson, R.P. (1964) What is watershed runoff?, J. Geophys. Res., 69, 1541-1552.

Beven, K.J. (1993) Prophecy, reality and uncertainty in distributed hydrological modeling, Advances in Water Resources, **16**, 41-51.

Beven, K. and Germann, P. (1982) Macropores and water flow in soils, Water Resour. Res., **18**, 1311-1325.

Beven, K. and Wood, F. (1983) Catchment geomorphology and the dynamics of runoff contributing areas, J. Hydrol., **65**, 139-158.

Beven, K. and Young, P.C. (1988) An aggregated mixing zone model of solute transport through porous media, J. Contam. Hydrol.,**3**, 129-143.

Beven, K.J, Lamb, R., Quinn, P., Romanowicz, R. and Freer, J. (1995) TOPMODEL, in Singh, V.P. (ed.), Computer models of watershed hydrology, Water Resources Publications, Colorado, 627-668.

Bonell, M. (1993) Progress in the understanding of runoff generation dynamics in forests, J. Hydrol., **150**, 217-275.

Bouma, J. (1981) Soil morphology and preferential flow along macropores, Agr. Water Manage., **3**, 235-250.

Brammer, D.D. and McDonell, J.J. (1996) An evolving perceptual model of hillslope flow at the Maimai catchment, in Anderson, M.G. and Brooks, S.M. (eds.), Advances in Hillslope Processes, John Wiley & Sons, New York, **1**, 35-60.

Brusseau, M.L. and Rao, P.S.C. (1990) Modeling solute transport in structured soils: a review, Geoderma, **46**, 169-192.

Buttle, J.M. and Peters, D.L. (1997) Inferring hydrological processes in a temperate basin using isotopic and geochemical hydrograph separation: a re-evaluation, Hydrol. Processes, **11**, 557-573.

Chen, C. and Wagenet, R.J. (1992) Simulation of water and chemicals in macropore soils. Part 1. Representation of the equivalent macropore influence and its effect on soil water flow, J. Hydrol., **130**, 105-126.

Chorley, R.J. (1978) The hillslope hydrological cycle, in Kirkby, M.J. (ed.), Hillslope hydrology, John Wiley & Sons, Chichester, UK, 1-42.

Christophersen, N., Neal, C., Hooper, R.P., Vog, R.D. and Andersen, S. (1990) Modeling stream water chemistry as a mixture of soil water end-members - a step towards second generation acidification models, J. Hydrol., 116, 307-320.

Church, M. and Woo, M.K. (1990) Geography of surface runoff: some lessons for research, in Anderson, M.G. and Burt, T.P. (eds.), Process studies in hillslope hydrology, John Wiley & Sons, Chichester, UK, 299-325.

Davidson, M.R. (1985) Numerical calculation of saturated-unsaturated infiltration in a cracked soil, Water Resour. Res., **21**, 709-714.

DeWalle, D.R., Swistock, B.R. and Sharpe, W.E. (1988) Three-component tracer model for stormflow on a small Appalachian forested catchment, J. Hydrol., **104**, 301-310.

Dietrich, W.E. and Dunne, T. (1978) Sediment budget for a small catchment in mountainous terrain, Z. Geomorphol. Suppl. Bd., **29**, 191-206.

Dunne, T. and Black, R.D. (1970) Partial area contributions to storm runoff in a small New England watershed, Water Resour. Res., **6**, 1296-1311.

Dunne, T. and Black, R.D. (1970) An experimental investigation of runoff production in permeable soils, Water Resour. Res., **6**, 478-490.

Dyson, J.S. and White, R.E. (1989) The effect of irrigation rate on solute transport in soil during steady water flow, J. Hydrol., **107**, 19-29.

Edwards, W.M., Shipitalo, M.J., Owens, L.B. and Norton, L.D. (1988) Contribution of macroporosity to infiltration into a continuous corn no-tilled watershed: Implications for contaminant movement, J. Contam. Hydrol., **3**, 193-205.

Edwards, W.M., Shipitalo, M.J., Owens, L.B. and Norton, L.D. (1989) Water and nitrate movement in earthworm burrows within long-term no-till cornfields, J. Soil & Water Conserv., **44**, 240-243.

Edwards, W.M., Shipitalo, M.J., Owens, L.B. and Norton, L.D. (1990) Effect of Lumbricus Terrestris L. burrows on hydrology of continuous no-till corn fields, Geoderma, **46**, 73-84.

Elsenbeer, H., West, A. and Bonell, M. (1994) Hydrological pathways and stormflow hydrochemistry at South Creek, northeast Queensland, J. Hydrol., **162**, 1-21.

Eshleman, K.N., Pollard, J.S. and O'Brien, A.K. (1993) Determination of contributing areas for saturation overland flow from chemical hydrograph separations, Water Resour. Res., **29**, 3577-3583.

Freeze, R.A. (1971) Three-dimensional, transient, saturated-unsaturated flow in a groundwater basin, Water Resour. Res., **7**, 347-366.

Freeze, R.A. (1972a) Role of subsurface flow in generating surface runoff. 1. Base flow contributions to channel flow, Water Resour. Res., **8**, 609-623.

Freeze, R.A. (1972b) Role of subsurface flow in generating surface runoff. 2. Upstream source areas, Water Resour. Res., **8**, 1272-1283.

Gaudet, J.P., Jégat, H., Vachaud, G. and Wierenga, P.J. (1977) Solute transfer, with exchange between mobile and stagnant water, through unsaturated sand, Soil Sci. Soc. Am. J., **41**, 665-671.

German, P.F. and Beven, K. (1985) Kinematic wave approximation to infiltration into soils with sorbing macropores, Water Resour. Res., 21, 990-996.

German, P.F. (1990) Macropores and hydrological hillslope processes, in Anderson, M.G. and Burt, T.P. (eds.), Process studies in hillslope hydrology, John Wiley, Chichester, 327-363.

Germann, P.F. (1991) Length scales of convection-dispersion approaches to flow and transport in porous media, J. Contam. Hydrol., **7**, 39-49.

Gillham, R.W. (1984) The effect of capillary fringe on water-table response, J. Hydrol., **67**, 307-324.

Gilman, K. (1971) A semi-quantitative study of the flow of natural pipes in the Nant Gerig sub-catchment, Subsurface Hydrology, Rep. no. 36, Inst. Hydrology, Wallingford, England.

Green, N.H. and Ampt, C.A. (1911) Flow of air and water through soils, J. Agric. Sci., **4**, 1-24.

Harr, R.D. (1977) Water flux in soil and subsoil on a steep forested slope, J. Hydrol., **33**, 37-58.

Hewlett, J.D. and Hibbert, A.R. (1967) Factors affecting the response of small watersheds to precipitation in humid areas, in Sopper, W.E. and Lull, H.W. (eds.), Proc. Int. Symp. on Forest Hydrology, Pergamon, New York, 275-290.

Hino, M., Ohta, T., Sunada, K. and Watanabe, K. (1989) Numerical methods in flood prediction – the 1st step, 252p., Morikita, Tokyo

Hornberger, G.M., Beven, K.J. and Germann, P.F. (1990)

Inferences about solute transport in macroporous forest soils from time series models, Geoderma, **46**, 249-262.

Hurley, D.G. and Pantelis, G. (1985) Unsaturated and saturated flow through a thin porous layer on a hillslope, Water Resour. Res., **21**, 821-824.

Ishihara, T. and Takasao, T. (1962) A study on the subsurface runoff and its effects on runoff process, Trans. of JSCE, **79**, 15-23 (in Japanese with English summary).

Jardine, P.M., Wilson, G.V. and Luxmoore, R.J. (1990) Unsaturated solute transport through a forest soil during rain storm events, Geoderma, **46**, 103-118.

Jones, A. (1971) Soil piping and stream channel initiation, Water Resour. Res., **7**, 602-610.

Jury, W.A. (1982) Simulation of solute transport using a transfer function model, Water Resour. Res., **18**, 363-368.

Jury, W.A. and Sposito, G. (1985) Field calibration and validation of solute transport models for the unsaturated zone, Soil Sci. Soc. Am. J., **49**, 1331-1341.

Kindaichi, H. (1988) Japanese, 1, 133-279, Iwanami, Tokyo (金田一春彦 , 日本語新版・上 , 岩波書店).

Kitahara, H., Shimizu, A. and Mashima, Y. (1988) Characteristics of pipe flow in a subsurface soil layer of a gentle hillside, J. Jpn. For. Soc., **70**, 318-323 (in Japanese with English summary).

Kitahara, H. and Nakai, Y. (1992) Relationship of pipe flow to streamflow on a first order watershed, J. Jpn. For. Soc., **74**, 49-54 (in Japanese with English summary).

Kitahara, H. (1993) Characteristics of pipe flow in forested slopes, IAHS Publ., **212**, 235-242.

Klute, A. (1952) A numerical method for solving the flow equation for water in unsaturated materials, Soil Sci., **73**, 105-116.

Kobayashi, D. (1985) Separation of the snowmelt hydrograph by stream temperatures, J. Hydrol., **76**, 155-162.

Kubota, J., Fukushima, Y. and Suzuki, M. (1987) Observation and modeling of the runoff processes on a hillslope, J. Jpn. For. Soc., **69**, 258-269.

Kubota, J., Fukushima, Y. and Suzuki, M. (1988) Observation and modeling of the runoff processes on a hillslope (II) Water budget and location of the groundwater table and its rising, J. Jpn. For. Soc., **70**, 381-389.

Kubota, J. and Sivapalan, M. (1995) Towards a catchment-scale model of subsurface runoff generation based on synthesis of small-scale process-based modeling and field studies, Hydrol. Processes, **9**, 541-554.

Luxmoore, R.J. (1981) Micro-, meso-, and macroporosity soil, Soil Sci. Soc. Am. J., **45**, 671-672.

Luxmoore, R.J., Jardine, P.M., Wilson, G.V., Jones, J.R. and Zelazny, L.W. (1990) Physical and chemical controls of preferred path flow through a forested hillslope, Geoderma, **46**, 139-154.

Matheron, G. and de Marsily, G. (1980) Is transport in porous media always diffusive? A counterexample, Water Resour. Res., **16**, 901-917.

McDonnell, J.J. (1990) A rationale for old water discharge through macropores in a steep, humid catchment, Water Resour. Res., **11**, 2821-2832.

McDonnell, J.J., Bonell, M., Stewart, M.K. and Pearce, A.J. (1990) Deuterium variations in storm rainfall: Implications for stream hydrograph separation, Water Resour. Res., **26**, 455-458.

McDonnell, J.J., Stewart, M.K. and Owens, I.F. (1991) Effect of catchment scale subsurface mixing on stream isotope response, Water Resour. Res., **27**, 3065-3073.

McDonnell, J., Brammer, D., Kendall, C., Hjerdi, N., Rowe, L., Stewart, M. and Woods, R. (1998) Flow pathways on steep forested hillslopes: The tracer, tensiometer and trough approach, in Sassa, K. (ed.), Environmental Forest Science (Proc. of IUFRO Div. 8 Conf., October 1998), Forestry Sciences vol. 54, Kyoto Univ., Japan, Kluwer Academic Publisher, Dordrecht, The Netherlands, 463-474.

Megahan, W.F. (1983) Hydrological effects of clearcutting and wildfire on steep granitic slopes in Idaho, Water Resour. Res., **19**, 811-819.

Misra, C., Nielsen, D.R. and Biggar, J.W. (1974) Nitrogen transformations in soil during leaching; I. Theoretical considerations, Soil Sci. Soc. Am. Proc., **38**, 289-293.

Moore, I.D., Grayson, R.B. and Ladson, A.R. (1991) Digital terrain modeling: A review of hydrological, geomorphological, and biological applications, Hydrol., Processes, **5**, 3-30.

National Land Agency (1988) Japan's New Comprehensive National Development Plan - Grand Design for the 21st Century, Ministry of Finance Printing Bureau, Tokyo (国土庁，新・全国総合開発計画「２１世紀の国土のグランドデザイン」)

Neuman, S.P. and Whitherspoon, P.A. (1971) Analysis of nonsteady flow with free surface using the finite element method, Water Resour. Res., **7**, 611-623.

Nielsen, D.R. and Biggar, J.W. (1962) Miscible displacement: III. Theoretical considerations, Soil Sci. Soc. Am. Proc., **26**, 216-221.

Noguchi, S., Tsuboyama, Y., Sidle, R.C. and Hosoda, I. (1997) Spatially distributed morphological characteristics of macropores in forest soils of Hitachi Ohta Experimental Watershed, Japan, J. For. Res., **2**, 207-215.

Noguchi, S., Tsuboyama, Y., Sidle, R.C. and Hosoda, I. (1999) Morphological characteristics of macropores and the distribution of preferential flow pathways in a forested slope segment, Soil Sci. Soc. Am. J., **63**, 1413-1423.

Noguchi, S., Tsuboyama, Y., Sidle, R.C. and Hosoda, I. (2001) Subsurface runoff characteristics from a forest hillslope soil profile including macropores, Hitachi Ohta, Japan, Hydrol. Processes, **15**, 2131-2149.

Ogawa, S., Kishi, Y. and Yamada, A. (1992) Studies on the infiltration-discharge of rain water and translation phenomena in soil, J. Hydrol., **132**, 1-23.

Ohta, T. (1988) Storm runoff mechanism on forested slopes, J. Jpn. Soc. Hydrol. & Water Resour., **1**, 75-82 (in Japanese with English summary).

Ohta, T. (1994) "Zero order basin" and forest hydrological researches -an outline of forest hydrology in Japan-, Proc. Int. Symp. on Forest Hydrology, University of Tokyo, 1-10.

Ohta, T. and Kido, T. (1986) Influence of evapo-transpiration of forests on slope discharge - Simulation of saturated-unsaturated throughflow using Richards' equation, J. Jpn. For. Soc., **68**, 490-498.

Oka, T. (1986) Rainfall infiltration and macropores in a hillside slope, Annuals Disas. Prev. Res. Inst., Kyoto Univ., No. **29**B-2, 279-289 (in Japanese with English summary).

Okunishi, K. and Iida, T. (1981) Evolution of hillslopes including landslides, Trans. Japanese Geomorphological Union, **2**, 291-299.

O'Loughlin, E. (1986) Prediction of surface saturation zones in natural catchments by topographic analysis, Water Resour. Res., **22**, 794-804.

Pearce, A.J. (1990) Streamflow generation processes: an Austral view, Water Resour. Res., **26**, 3037-3047.

Pearce, A.J., Stewart, M.K. and Sklash, M.G. (1986) Storm runoff generation in humid headwater catchments, 1. Where does the water come from?, Water Resour. Res., **22**, 1263-1272.

Philip, J.R. (1957) The theory of infiltration. 4. Sorptivity and algebraic infiltration equations, Soil Sci., **84**, 257-264.

Pierson, T.C. (1980) Piezometric response to rainstorms in forested hillslope drainage depressions, J. Hydrol. (New Zealand), **19**, 1-10.

Pond, S.F. (1971) Qualitative investigation into the nature and distribution of flow processes in Nant Gerig, Subsurface Hydrology, Rep. No. 28, Inst. Hydrology, Wallingford, England.

Richards, L.A. (1931) Capillary conduction of liquids through porous media, Physics **1**, 318-333.

Rose, D.A. and Passioura, J.B. (1971) The analysis of experiments on hydrodynamic dispersion, Soil Sci., **111**(4), 252-257.

Roth, K., Jury, W.A., Flühler, H. and Attinger, W. (1991) Transport of chloride through an unsaturated field soil, Water Resour. Res., **27**, 2533-2541.

Schoeneberger, P. and Amoozegar, A. (1990) Directional saturated hydraulic conductivity and macropore morphology of a soil-saprolite sequence, Geoderma, **46**, 31-49.

Sharma, M.L., Luxmoore, R.J., DeAngelis, R., Ward, R.C. and Yeh, G.T. (1987) Subsurface water flow simulated for hillslopes with spatially dependent soil hydraulic characteristics, Water Resour. Res., **23**, 1523-1530.

Shiraki, K. (1998) A new method for simulating water flow in hillslope soils using coarse space grids, J. Jap. Soc. Hydrol. & Water Resour., **11**(6), 586-598.

Sidle, R.C., Kardos, L.T. and van Genuchten, M.Th. (1977) Heavy metals transport model in a sludge-treated soil, J. Environ. Qual., **6**, 438-443.

Sidle, R.C. and Kardos, L.T. (1979) Nitrate leaching in a sludge-treated forest soil, Soil Sci. Soc. Am. J., **43**, 278-282.

Sidle, R.C. (1984) Shallow groundwater fluctuations in unstable hillslopes of coastal Alaska, Z. für Gletscherkunde und Glazialgeol., **20**, 79-95.

Sidle, R.C., Pearce, A.J. and O`Loughlin, C.L. (1985) Hillslope Stability and Land Use, Water Resour. Mono. 11, Am. Geophys. Union, Wash., D.C., p140.

Sidle, R.C. and Tsuboyama, Y. (1992) A comparison of piezometric response in unchanneled hillslope hollows: coastal Alaska and Japan, J. Japan Soc. Hydrol. & Water Resour., **5**, 3-11.

Sidle, R.C., Tsuboyama, Y., Noguchi, S., Hosoda, I., Fujieda, M. and Shimizu, T. (1995) Seasonal hydrological response at various spatial scales in a small forested catchment, Hitachi Ohta, Japan, J. Hydrol., **168**, 227-250.

Sidle, R.C., Tsuboyama, Y., Noguchi, S., Hosoda, I., Fujieda, M. and Shimizu, T. (2000) Stormflow generation in steep forested headwaters: a linked hydrogeomorphic paradigm, Hydrol. Processes, **14**, 369-385.

Sidle, R.C., Noguchi, S., Tsuboyama, Y. and Laursen, K. (2001) A conceptual model of preferential flow systems in forested hillslopes: evidence of self-organization, Hydrol. Processes, **15**, 1675-1692.

Sklash, M.G. (1990) Environmental isotope studies of storm and snowmelt runoff generation, in Anderson, M.G. and Burt, T.P. (eds.), Process studies in hillslope hydrology, John Wiley, New York, 401-435.

Sklash, M.G., Stewart, M.K. and Pearce, A.J. (1986) Storm runoff generation in humid headwater catchments 2. A case study of hillslope and low-order stream response, Water Resour. Res., **22**, 1273-1282.

Sloan, P.G. and Moore, I.D. (1984) Modeling subsurface stormflow on steeply sloping forested watersheds, Water Resour. Res., **20**, 1815-1822.

Smith, R.E. and Hebbert, R.H.B. (1983) Mathematical simulation of interdependent surface and subsurface hydrological processes, Water Resour. Res., **19**, 987-1001.

Stallman, R.W. (1965) Steady one-dimensional fluid flow in a semi-infinite porous medium with sinusoidal surface temperature, J. Geophys. Res., **70**, 2821-2827.

Stewart, M.K. and McDonell, J.J. (1991) Modeling base flow soil water residence times from deuterium concentrations, Water Resour. Res., **27**, 2681-2693.

Suzuki, M. (1984a) The properties of a base-flow recession on small mountainous watersheds (I) Numerical analysis using the saturated-unsaturated flow model, J. Jap. For. Soc., **66,** 174-182. (in Japanese with English summary)

Suzuki, M. (1984b) The properties of a base-flow recession on small mountainous watersheds (II) Influence of evapotranspiration on recession hydrographs, J. Jap. For. Soc., **66**, 211-218

Suzuki, S. (1960) Percolation measurements based on heat flow through soil with special reference to paddy fields, J. Geophys. Res., **65**, 2883-2885.

Takahashi Y (ed.) (1982) Water, vol. **1**, 73-77, Gihoudo, Tokyo (高橋裕編 , 水のはなしⅠ , 技報堂出版 , 東京).

Takasao, T., Shiiba, M. and Zhang, S. (1986) A coupled runoff model of surface flow and subsurface flow, Annuals Disas. Prev. Res. Inst., Kyoto Univ., No. **29**B-2, 253-269.

Tanaka, T. (1982) The role of subsurface water exfiltration in soil erosion processes, IAHS/AISH Publ., **137**, 73-80.

Tanaka, T., Yasuhara, M., Sakai, H. and Marui, A. (1988) The Hachioji Experimental Basin study - storm runoff processes and the mechanisms of its generation, J. Hydrol., **102**, 139-164.

Tani, M. (1982) The properties of a water-table rise produced by a one-dimensional, vertical, unsaturated flow, J. Jap. For. Soc., **64**, 409-418 (in Japanese with English summary).

Tani, M. (1985) Analysis of one-dimensional, vertical, unsaturated flow in consideration of runoff properties of a mountainous watershed, J. Jap. For. Soc., **67**, 449-460 (in Japanese with English summary).

Torres, R., Dietrich, W.E., Montgomery, D.R., Anderson, S.P. and Loague, K. (1998) Unsaturated zone processes and the hydrological response of a steep, unchanneled catchment, Water Resour. Res., **34**, 1865-1879.

Troch, P.A., De Troch, F.P. and Brutsaert, W. (1993) Effective water table depth to describe initial conditions prior to storm rainfall in humid regions, Water Resour. Res., **29**(2), 427-434

Tsuboyama, Y. and Sammori, T. (1989) Numerical simulation of seepage in a forested hillslope by finite element method, J. Jap. Soc. Hydrol. & Water Resour., **2**, 49-56.

Tsuboyama, Y., Hosoda, I., Noguchi, S. and Sidle, R.C. (1994a) Piezometric response in a zero-order basin, Hitachi Ohta, Japan, in Ohta, T. (ed.), Proc. Int. Symp. on Forest Hydrology, Univ. of Tokyo, Japan, 217-224.

Tsuboyama, Y., Sidle, R.C., Noguchi, S. and Hosoda, I. (1994b) Flow and solute transport through the soil matrix and macropores of a hillslope segment, Water Resour. Res., **30**, 879-890.

Tsuboyama, Y., Noguchi, S., Shimizu T, Sidle, R.C. and Hosoda. I (1998) Intrastorm fluctuations of piezometric head and soil temperature within a steep forested hollow, in Sassa, K. (ed.), Environmental Forest Science (Proc of IUFRO Div 8 Conf., October 1998), Forestry Sciences vol. 54, Kyoto Univ., Japan, Kluwer Academic Publisher, Dordrecht, The Netherlands, 475-482.

Tsuboyama, Y., Sidle, R.C., Noguchi, S., Murakami, S. and Shimizu, T. (2000) A zero-order basin – its contribution to catchment hydrology and internal hydrological processes, Hydrol. Processes, **14**, 387-401

Tsukamoto, Y. (1963) Storm discharge from an experimental watershed, J. Jpn. Soc. For., **45**(6), 186-190.

Tsukamoto, Y. (1973) On some characteristics of rainfall-induced landslides, Proc. of 10th General Symposium on Disaster Sciences, 303-306 (塚本良則 , 豪雨型山崩れにみられる２，３の特性について , 第 10 回災害科学総合シンポジウム).

Tsukamoto, Y., Ohta, T. and Noguchi, H. (1982) Hydrological and geomorphological studies of debris slides on forested hillslopes in Japan, IAHS Publ., 137, 89-98.

Tsukamoto, Y. and Ohta, T. (1988) Runoff process on a steep forested slope, J. Hydrol., **102**, 165-178.

Uchida, T., Kosugi, K., Kobashi, S. and Mizuyama, T. (1995) Observation and survey of underground pipes at Toinotani basin in Ashu experimental forest, Bull. Kyoto Univ. For., **67**, 58-67 (in Japanese with English summary).

van Genuchten, M.Th. (1980) A closed-form equation for predicting the hydraulic conductivity of unsaturated soils, Soil Sci. Soc. Am. J., **44**, 892-898.

van Genuchten, M.Th. and Wierenga, P.J. (1986) Solute dispersion coefficients and retardation factors, in Methods of Soil Analysis, Part I. Physical and Mineralogical Methods, Agronomy Monograph no. 9 (2nd ed.), American Society of Agronomy, Madison, Wisc. , 1025-1054.

Wang, D., Kubota, J. and Tsukamoto, Y. (1993) The role of vertical pipes in the formation of saturated zones in a hillslope, J. Jpn. For. Soc., **75**, 88-99 (in Japanese with English summary).

Whipkey, R.Z. and Kirkby, M.J. (1978) Flow within the soil, in Kirkby, M.J. (ed.), Hillslope Hydrology, John Wiley & Sons, Chichester, UK, 121-144.

White, R.E., Dyson, J.S., Haigh, R.A., Jury, W.A. and Sposito, G. (1986) A transfer function model of solute transport through soil 2. Illustrative applications, Water Resour. Res., **22**, 248-254.

Wilson, G.V., Jardine, P.M., Luxmoore, R.J. and Jones, J.R. (1990) Hydrology of a forested hillslope during storm events, Geoderma, **46**, 119-138.

Wilson, G.V., Jardine, P.M., Luxmoore, R.J., Zelazny, L.W., Lietzke, D.A. and Tod, D.E. (1991a) Hydrogeochemical processes controlling subsurface transport from an upper subcatchment of Walker Branch watershed during storm events. 1. Hydrological transport processes, J. Hydrol., **123**, 297-316.

Wilson, G.V., Jardine, P.M., Luxmoore, R.J., Zelazny, L.W., Tod, D.E. and Lietzke, D.A. (1991b) Hydrogeochemical processes controlling subsurface transport from an upper subcatchment of Walker Branch watershed during storm events. 2. Solute transport processes, J. Hydrol., **123**, 317-336.

Yamamoto, S. (1972) Outline of Hydrology, Kyoritu Shuppan, Tokyo, 1-38 (山本荘毅，水文学総論，共立出版，東京).

Yamagami, T. (1977) A study on the finite element solution of transient seepage under drawdown, Trans. of JSCE, **263**, 85-95 (in Japanese)

Yasuhara, M. and Marui, A. (1994) Groundwater discharge from a clayey hillslope, in Ohta, T. (ed.), Proc Int. Symp. on Forest Hydrology, Univ. of Tokyo, Japan, 241-248.

Ziemer, R.R. (1992) Effect of logging on subsurface pipeflow and erosion: coastal northern California, USA, IAHS Publ., **209**, 187-197.

Zienkiewicz, O.C. and Taylor, R.L. (1989) Finite element method fourth edition. Volume 1. Basic formulation and linear problems, McGraw-Hill, London, 260-289.

森林小流域における雨水流動経路の変動特性に関する研究

坪山 良夫 [1)*]

要 旨

森林小流域における雨水流動経路について、土壌断面からの流出測定、塩素イオンをトレーサとする混合置き換え実験、０次谷における流出・間隙水圧・地温の観測、小流域全体の水文観測等、複数スケールにわたる系統的な現地調査を行った。その結果、地中の水移動経路と流出発生域の変動という二つの異なるスケールで起きる現象に共通する特徴として、マクロポアや０次谷のような潜在的な水みちが実際の雨水流動経路として機能するには一定量の先行水分が必要であり、一度その閾値を越えると、それ自体の集水空間が増えることによって雨水流動経路としての機能がいっそう高まり、より大きなスケールでの流出への相対的な寄与が増大することが明らかになった。

キーワード：流域水文、０次谷、山腹斜面、土壌断面、マクロポア、トレーサ

＊森林総合研究所水土保全研究領域　〒 305-8687　茨城県つくば市松の里 1　e-mail: tsubo@ffpri.affrc.go.jp
1) 森林総合研究所水土保全研究領域